Applied Geochemistry 24 (2009) 191–207

Contents lists available at ScienceDirect

Applied Geochemistry

journal homepage: www.elsevier.com/locate/apgeochem

Sulfur geochemistry of hydrothermal waters in Yellowstone National Park: IV Acid–sulfate waters

D. Kirk Nordstrom *, R. Blaine McCleskey, James W. Ball

US Geological Survey, Boulder, CO 80303, USA

ARTICLE INFO

Article history:
Available online 24 November 2008

ABSTRACT

Many waters sampled in Yellowstone National Park, both high-temperature (30–94 °C) and low-temperature (0–30 °C), are acid–sulfate type with pH values of 1–5. Sulfuric acid is the dominant component, especially as pH values decrease below 3, and it forms from the oxidation of elemental S whose origin is H_2S in hot gases derived from boiling of hydrothermal waters at depth. Four determinations of pH were obtained: (1) field pH at field temperature, (2) laboratory pH at laboratory temperature, (3) pH based on acidity titration, and (4) pH based on charge imbalance (at both laboratory and field temperatures). Laboratory pH, charge imbalance pH (at laboratory temperature), and acidity pH were in close agreement for pH < 2.7. Field pH measurements were predominantly used because the charge imbalance was <±10%. When the charge imbalance was generally >±10%, a selection process was used to compare acidity, laboratory, and charge balance pH to arrive at the best estimate. Differences between laboratory and field pH can be explained based on Fe oxidation, H_2S or S_2O_3 oxidation, CO_2 degassing, and the temperature-dependence of pK_2 for H_2SO_4. Charge imbalances are shown to be dependent on a speciation model for pH values <3. The highest SO_4 concentrations, in the thousands of mg/L, result from evaporative concentration at elevated temperatures as shown by the consistently high $\delta^{18}O$ values (−10‰ to −3‰) and a δD vs. $\delta^{18}O$ slope of 3, reflecting kinetic fractionation. Low SO_4 concentrations (<100 mg/L) for thermal waters (>350 mg/L Cl) decrease as the Cl^- concentration increases from boiling which appears inconsistent with the hypothesis of H_2S oxidation as a source of hydrothermal SO_4. This trend is consistent with the alternate hypothesis of anhydrite solubility equilibrium. Acid–sulfate water analyses are occasionally high in As, Hg, and NH_3 concentrations but in contrast to acid mine waters they are low to below detection in Cu, Zn, Cd, and Pb concentrations. Even concentrations of SO_4, Fe, and Al are much lower in thermal waters than acid mine waters of the same pH. This difference in water chemistry may explain why certain species of fly larvae live comfortably in Yellowstone's acid waters but have not been observed in acid rock drainage of the same pH.

Published by Elsevier Ltd.

1. Introduction

The thermal features of Yellowstone National Park have been largely inventoried by the National Park Service and more than 10,000 features are compiled in a database (Rodman and Guiles, 2008). A large proportion of these features are acidic from H_2SO_4 produced by microbial S oxidation in near-surface environments. Three previous papers have discussed the occurrence of intermediate S species, especially thiosulfate (Xu et al., 1998, 2000; Druschel et al., 2003). The purpose of this paper is to present detailed chemistry of the acid–sulfate waters at Yellowstone, interpret their formation, and document some of their biological activity. Although several of these aspects have been reported in the literature previously, the large quantity of high-quality analytical data has not been available, nor have these data been interpreted in terms of the larger picture of naturally occurring acidic waters. Occasional comments will point out the difference between Yellowstone's acid waters and acid rock drainage of similar pH values.

2. Sampling locations

Water samples were collected from Mammoth Hot Springs, Norris Geyser Basin, Upper, Lower, and Midway Geyser Basins, Gibbon Geyser Basin, Potts Hot Spring Basin, West Thumb Geyser Basin, Hot Spring Basin, Coffee Pot Springs, Rainbow Springs, Josephs Coat Hot Springs, Shoshone Geyser Basin, Heart Lake Geyser Basin, and Brimstone Basin. These locations are shown in Fig. 1. The majority of acid samples come from Norris Geyser Basin but by including data from other basins, the coverage is broad and includes samples from inside and outside the caldera boundary, from a variety of major rock types, and having a wide range of pH,

* Corresponding author.
E-mail address: dkn@usgs.gov (D. Kirk Nordstrom).

0883-2927/$ - see front matter Published by Elsevier Ltd.
doi:10.1016/j.apgeochem.2008.11.019

Fig. 1. Map of Yellowstone National Park showing the main areas of sample collection with solid circles. Most acid waters are found in or near Norris Geyser Basin or Brimstone Basin. Dashed line follows caldera boundary.

temperature, and composition. This broad range of high-quality analyses allows a better examination of geothermal water types and their origins and distribution.

3. Sample collection and preservation

Springs and geysers were sampled as close to the discharge source as possible. Extreme care was taken to safely collect water samples from the larger geothermal sites, to protect fragile hot-spring mineral formations, and to minimize changes in temperature, pH, and water chemistry during sampling. Samples were collected from the middle of large pools and geysers by positioning the sample tubing intake using an insulated stainless-steel container as a flotation device attached to the end of an extendable Al pole. At more easily accessible sites, the tubing intake was positioned in the source or channel by hand. A Teflon block attached to the end of the sampling tubing was used as a weight to keep the sample tubing in place (McCleskey et al., 2005). Grab samples also were collected from the source using the stainless-steel container or a syringe fitted with Teflon tubing.

Samples were collected and filtered on-site by either or both of two techniques. The first technique consisted of pumping the water directly from the source with a battery-operated peristaltic pump fitted with medical-grade silicone tubing through a 142-mm diameter all-plastic filter holder (Kennedy et al., 1976) containing a 0.1-μm pore size mixed-cellulose–ester filter membrane. The second technique consisted of filling a 60-mL syringe by suctioning from the source or with source water collected in the stainless-steel container and immediately forcing the water through a 25-mm disposable filter having a mixed-cellulose–ester membrane with a pore size of 0.2- or 0.45-μm.

Sample splits were collected for analyses of inorganic constituents, redox species, stable water isotopes (δD and $\delta^{18}O$), and dissolved organic C (DOC). Container preparation and storage and stabilization methods for filtered samples are summarized in Table 1. Samples for the determination of major cations and trace elements (As, Al, B, Ba, Be, Ca, Cd, Co, Cr, Cu, Fe, Hg, K, Li, Mg, Mn, Mo, Na, Ni, Pb, Sb, Se, SiO_2, Sr, V, and Zn), major anions (Br, Cl, F, NO_3, and SO_4), alkalinity (HCO_3), acidity, density, NH_4, NO_2, DOC, and water isotopes were filtered and then stabilizing reagents, if

Table 1
Container preparation and stabilization methods for filtered samples. All preservative reagents were added in the field except where otherwise noted.

Sample type(s)	Storage container and preparation	Stabilization treatment in addition to refrigeration
Major cations and trace elements (Al, B, Ba, Be, Ca, Cd, Co, Cr, Cu, K, Li, Mg, Mn, Mo, Na, Ni, Pb, Sb, Se, SiO_2, Sr, V, and Zn)	Polyethylene bottles, soaked in 5% HCl and rinsed three times with distilled water	1% (v/v) concentrated redistilled HNO_3 added, samples were not chilled
Total Hg(Hg(T))	Borosilicate glass bottles, soaked with 5% HNO_3 and rinsed three times with deionized water	5 mL of concentrated redistilled HNO_3 (added in the field) + 0.04% w/v $K_2Cr_20_7$ per 125 mL of sample (added in the laboratory)
Methyl Hg (CH_3Hg)	Teflon bottles, double-bagged and transported containing about 100 mL 5% HCl	5 mL 6 M redistilled HCl added
Fe and As redox species (Fe(T), Fe(II), As(T), and As(III))	Opaque polyethylene bottles, soaked in 5% HCl and rinsed three times with distilled water	1% (v/v) redistilled 6 N HCl added
Major anions (Br, Cl, F, NO_3, and SO_4), alkalinity as HCO_3, acidity, density, and NO_2	Polyethylene bottles filled with distilled water and allowed to stand for 24 h, then rinsed three times with distilled water	None
NH_4	Same as major cations and trace metals	l%(v/v) 1:9H_2SO_4 added
SiO_2	Same as major anions, alkalinity, and density	1 mL diluted to 25 mL with distilled water on-site
Thiosulfate and polythionate (S_2O_3, S_nO_6)	30-mL polyethylene bottle	1.7% (v/v) 0.6 M $ZnCl_2$ plus 1% (v/v) 1 M NaOH added; 1.7% (v/v) 1 M KCN also added to S_nO_6 bottle
Dissolved organic carbon (DOC)	Amber glass bottle baked at 600 °C	None
Water Isotopes (6D and $\delta^{18}O$)	60-mL glass bottle	None (unfiltered sample collected when filtration was not possible)

needed, were added. Sample bottles were pre-rinsed with filtered water prior to sample collection. Stabilizing reagents for intermediate S species were put into the sample bottle before the sample was collected; therefore, these bottles were not pre-rinsed. With the exception of the cation sample, all sample splits were chilled as soon as practical after sample collection. Laboratory measurements of pH and specific conductance were made weeks later on the filtered anion samples after equilibrating with air.

To prevent over-estimation of S_2O_3 concentrations, S(-II) oxidation was minimized by adding $ZnCl_2$. This technique caused the oxidation-resistant ZnS species to precipitate. Polythionate (S_nO_6) was converted to thiocyanate (SCN) by the addition of KCN to that sample split (Moses et al., 1984). For the analysis of dissolved SiO_2 in waters from hot springs and geysers, 1 mL of filtered sample was diluted on-site to 25 mL with distilled water to prevent the precipitation of SiO_2 as the sample cooled. Samples for the determination of DOC were filtered through a 142-mm diameter all-plastic plate filter containing a 0.1-μm mixed-cellulose-ester filter membrane and collected in an amber glass bottle that had been baked at 600 °C. At least 1 L of sample water was passed through the all-plastic plate-filter assembly before a DOC sample was collected. Samples for water isotope determinations were filtered when the water filtered easily; otherwise water-isotope samples were not filtered.

4. Analytical methods

4.1. Field measurements

Measurements of electromotive force, or redox potential, (EMF), pH, temperature, specific conductance, and H_2S were performed on-site. Measurements of EMF were checked against ZoBell's solution at the beginning of each day (Nordstrom, 1977). Measurements of EMF and pH were made on unfiltered sample water pumped from the source through an acrylic plastic flow-through cell which minimized sample contact with air. The flow-through cell contained a combination redox electrode, a pH electrode with integral thermistor, and test tubes containing buffer solutions for calibration of the pH electrode. Flow velocities in the flow-cell were too low for streaming potentials to affect the electrodes. All components were thermally equilibrated with the sample water before obtaining measurements. Where possible, temperature and specific conductance measurements were made by immersing probes directly into the source as close to the sampling point as possible. Otherwise, probes were immersed into an unfiltered sample collected in a stainless-steel insulated container, or into the flow-through cell. Conversion of EMF to Eh (redox potential relative to the standard hydrogen electrode) was made using the EMF of the half-cell reference potential for the Orion Pt combination electrode at the temperature of the measurement (see Nordstrom, 1977).

A mobile laboratory truck containing an ion chromatograph, ultraviolet–visible spectrophotometer, autotitrator, and reagent-grade water system was set up so that unstable intermediate S oxyanion species could be determined as soon as possible after sample collection. Iron redox species also were determined in the mobile laboratory to guide sampling strategies. Alkalinity and acidity titrations were performed sometimes within a few days in the field, sometimes back at the USGS Boulder laboratory facilities, but always before oxidation and hydrolysis reactions occurred.

Field measurement of pH in geothermal waters is challenging because of high-temperatures, complex sample matrices often supersaturated with CO_2, and surging water resulting from gas discharge. Because many pH electrodes perform poorly in near-boiling water, electrodes rated for boiling or near-boiling water temperatures were used. All electrodes were glass combination and most were Orion or Thermo Orion Ross combination electrodes. At each site, the flow-through cell, temperature probe, electrode, and calibration buffers were equilibrated to sample temperature prior to calibration and measurement. The system was calibrated using at least two bracketing standard buffers (chosen from among 1.68, 2.00, 4.01, 7.00, or 10.00) corrected to their values at the sample temperature. After calibration, the pH electrode was placed in the sample water in the flow-through cell and monitored until no change in temperature (±0.1 °C) or pH (±0.01 standard unit) was detected for at least 30 s. Following sample measurement, the electrode was re-immersed in the standard buffer of pH closest to that of the sample and allowed to equilibrate. The entire calibration and measurement process was repeated as many times as necessary until the measured value for the buffer differed by no more than 0.05 standard units from its certified pH at the measured temperature.

Dissolved H_2S concentration was measured on-site using a battery operated, portable ultraviolet–visible spectrophotometer and the methylene blue method (equivalent to Standard Method

4500-S^{2-} D for waste water; APHA, 1985). To minimize the inclusion of atmospheric air, samples for H_2S determination were either collected directly from the outflow of a thoroughly equilibrated 142-mm plastic filter with a 0.1-μm membrane filter, or drawn into a plastic syringe fitted with about 25 cm of Teflon tubing flushed at least three times with sample fluid and forced through a syringe-mounted 0.2-μm or 0.45-μm membrane filter. Samples were filtered directly into a measuring cuvette and color reagents were added immediately. After waiting for color development, the sample absorbance and temperature of the solution were measured.

4.2. Laboratory methods

Several different methods and different laboratories were used to achieve the results given in the following tables. Most of the details for analytical methods can be found in the respective reports. Table 2 summarizes these techniques and shows to which reports they pertain.

4.3. Water stable isotopes

Hydrogen isotope ratios were determined using a hydrogen equilibration technique (Coplen et al., 1991; Revesz and Coplen, 2003a). Oxygen isotope ratios were determined using the CO_2 equilibration technique of Epstein and Mayeda (1953), which has been automated by Revesz and Coplen (2003b). The isotopic concentration is reported in the standard "delta notation"

$$\delta^{18}O‰ = \frac{(^{18}O/^{16}O)_{sample} - (^{18}O/^{16}O)_{standard}}{(^{18}O/^{16}O)_{standard}} \times 1000 \quad (1)$$

where ‰ is per mil.

Oxygen and H isotopic results are reported relative to the standard VSMOW (Vienna Standard Mean Ocean Water) and normalized (Coplen, 1994) on scales such that the O and H isotopic values of SLAP (Standard Light Antarctic Precipitation) are −55.5‰ and −428‰, respectively.

4.4. Acidity determinations

Total acidity was determined at the USGS laboratory in Boulder, Colorado by titrating samples having a pH less than 5 to a pH greater than 7 using an autotitrator and standardized NaOH solution. The NaOH titrant (0.01–0.05 M) was standardized daily by titrating a known quantity of potassium hydrogen phthalate ($KHC_8H_4O_4$). The titrator was programmed for 50- to 100-μL constant-volume additions or constant change in millivolts (mV), typically 10 mV per addition. Equivalence points were determined using a modified Gran's function (Barringer and Johnsson, 1996)

$$F_{acid} = (v_0 + v_{NaOH}) \times 10^{-pOH} \quad (2)$$

where F_{acid} = the Gran function, v_0 = sample volume, v_{NaOH} = volume of NaOH titrant added, and pOH = 14 minus pH.

Acidity is occasionally determined in acid mine waters, but not commonly in other waters. In addition to H^+, the principal components contributing to acidity are HSO_4^-, CO_2 and hydrolyzable metals (Kirby and Cravotta, 2005a, b). The contributions of As and F

Table 2
Analytical methods used for each data report and method references.

Constituents and methods	Method references	Data report
Cations/trace metals		
DCP-AES	Johnson et al. (1979) and Ball and Nordstrom (1994)	96T, 98Ba
ICP-AES	Garbarino and Taylor (1979)	98Bb, 01B, 02B, 05M, 07B, 07T
FAAS	Taylor (1978)	96T, 98Ba, 98Bb, 01B, 02B, 02K
GFAAS	Taylor (1978)	98Bb, 01B, 02B, 05M, 07B
ICP-MS	Taylor (2001)	02K, 07T
As speciation		
HGAAS	McCleskey et al. (2003)	01B, 02B, 05M, 07B, 07T
Colorimetric	Johnson and Pilson (1972)	98Ba
Fe speciation		
Colorimetric	Stookey (1970) and To et al. (1999)	98Ba, 98Bb, 01B, 02B, 05M, 07B, 07T
Hg		
CVAAS	Taylor et al. (1997) and Roth et al. (2001)	05M, 07B
CH_3Hg		
CVAAS	Horvat et al. (2003); DeWild et al. (2002)	07B
H_2S		
Colorimetric	American Public Health Association (1985)	98Bb, 01B, 02B, 05M, 07B, 07T
ISE	Baumann (1974)	98Ba
Titration	Fishman and Friedman (1985)	96T
Anions		
IC (F, Cl, Br, NO_3, SO_4)	Brinton et al. (1995)	96T, 98Ba, 98Bb, 01B, 02B, 02K, 05M, 07B, 07T
ISE (F)	Barnard and Nordstrom (1980_	96T, 98Bb, 01B, 02B, 05M, 07B
Thorin (SO_4)	Brown et al. (1970)	96T
Turbidimteric (SO_4)	Fishman and Friedman (1985)	96T
IC (S_2O_3)	Moses et al. (1984)	98Bb, 01B, 02B, 05M, 07B, 07T
Alkalinity titration	Barringer and Johnsson (1996)	96T, 98Ba, 98Bb, 01B, 02B, 02K, 05M, 07B, 07T
Acidity titration	Barringer and Johnsson (1996)	96T, 01B, 02B, 05M, 07B
Isotopes	Coplen et al. (1991)	96T, 98Bb, 01B, 02K, 02B, 05M, 07B, 07T
MS	Epstein and Mayeda (1953)	

96T Thompson and DeMonge (1996).
98Ba Ball et al. (1998a).
98Bb Ball et al. (1998b).
01B Ball et al. (2001).
02B Ball et al. (2002).
02K Kharaka et al. (2002).
05M McCleskey et al. (2005).
07B Ball et al. (2007).
07T Takacs-Vesbach, written communication.

also should be considered for geothermal waters, because their concentrations sometimes exceed Fe or Al concentrations under mildly acidic conditions (Ball et al., 2002; McCleskey et al., 2005). Arsenic(III) remains fully protonated (undissociated) up to pH 9 and cannot contribute to the acidity. Arsenic(V), however, has a $pK_1 = 2.3$ and $pK_2 = 7$. Thus, of the As hydrolysis species only the $H_2ASO_4^-$ intermediate hydrolysis species need be considered for the hydrolysis correction. Although occasionally present at concentrations exceeding 500 mg/L in geothermal waters (McCleskey et al., 2005), NH_3 need not be considered because $pK = 9.25$ for the deprotonation of NH_4^+. Thus, the important reactions contributing to total acidity in geothermal waters are HSO_4^- dissociation, Fe oxidation and hydrolysis, Al hydrolysis, $H_3AsO_4^0$ dissociation, and HF^0 dissociation, according to the following reactions (pK values from Nordstrom and Munoz, 1994; Nordstrom and Archer, 2003):

$$HSO_4^- \leftrightarrow H^+ + SO_4^{2-} \quad (pK = 1.98) \tag{3}$$

$$Fe^{2+} + 1/4O_2 + H^+ \leftrightarrow Fe^{3+} + 1/2H_2O \quad (pK = -7.77) \tag{4}$$

$$Fe^{3+} + H_2O \leftrightarrow FeOH^{2+} + H^+ \quad (pK_1 = 2.19) \tag{5}$$

$$FeOH^{2+} + H_2O \leftrightarrow Fe(OH)_2^+ + H^+ \quad (pK_2 = 3.48) \tag{6}$$

$$Fe(OH)_2^+ + H_2O \leftrightarrow Fe(OH)_3^0 + H^+ \quad (pK_3 = 6.93) \tag{7}$$

$$Al^{3+} + H_2O \leftrightarrow AlOH^{2+} + H^+ \quad (pK_1 = 5.00) \tag{8}$$

$$AlOH^{2+} + H_2O \leftrightarrow Al(OH)_2^+ + H^+ \quad (pK_2 = 5.10) \tag{9}$$

$$Al(OH)_2^+ + H_2O \leftrightarrow Al(OH)_3^0 + H^+ \quad (pK_3 = 6.70) \tag{10}$$

$$H_3AsO_4^o \leftrightarrow H_2AsO_4^- + H^+ \quad (pK_1 = 2.30) \tag{11}$$

$$H_2AsO_4^- \leftrightarrow HAsO_4^{2-} + H^+ \quad (pK_2 = 6.99) \tag{12}$$

$$HF^o \leftrightarrow H^+ + F^- \quad (pK_1 = 3.18) \tag{13}$$

Because contributions from the above hydrolysis and dissociation reactions must be subtracted from the total acidity, the value obtained for free H^+ acidity is model-dependent. For Fe(II) oxidation, Eqs. (4) and (5) approximately cancel each other, because (4) consumes a proton, and (5) generates one. Thus, assuming complete oxidation of Fe(II) during the acidity titration, dissolved Fe(II) can be treated as $FeOH^{2+}$ for the purpose of calculating H^+ acidity. Although usually less than about 2 mg/L at pH < 3, F concentrations can approach 10 mg/L in mildly acidic geothermal waters (McCleskey et al., 2005). Although the concentration of the HF° aqueous complex becomes greater than that of free F^- at pH < 3.2, the predominant F complexes typically are with Al.

Free H^+ was derived from the total acidity by subtracting the H^+ ions produced by hydrolysis of Fe^{3+} and Al^{3+} ions, and dissociation of HSO_4^-, $H_3AsO_4^0$ and HF^0, as calculated by PHREEQCi, a graphical-user-interface version (Charlton et al., 1997) of program PHREEQC (Parkhurst and Appelo, 1999) incorporating the WATEQ4F database, as follows:

$$Acidity_{SO_4} = HSO_4^- \tag{14}$$

$$Acidity_{Fe} = 3(Fe^{III}(tot) - FeOH^{2+} - Fe(OH)_2^+) + 2FeOH^{2+} + Fe(OH)_2^+ + 2Fe^{II}(tot) \tag{15}$$

$$Acidity_{Al} = 3(Al(tot) - AlOH^{2+} - Al(OH)_2^+) + 2AlOH^{2+} + Al(OH)_2^+ \tag{16}$$

$$Acidity_{As} = 2(As^V(tot) - H_2AsO_4^-) + H_2AsO_4^- \tag{17}$$

$$Acidity_F = HF^0 \tag{18}$$

$$Acidity_{H^+} = Acidity_{Total} - Acidity_{SO_4} - Acidity_{Fe} - Acidity_{Al} - Acidity_{As} - Acidity_F \tag{19}$$

It is implicitly assumed that divalent Fe is entirely present as free Fe^{2+} ion, which is consistent with the high pK value of the hydrolysis reaction:

$$Fe^{2+} + H_2O \leftrightarrow FeOH^+ + H^+ \quad (pK = 9.5) \tag{20}$$

Concentrations for the above equations are expressed in moles/kg of water. Sample pH from the acidity titration (acidity pH) was calculated by computing the product of the H^+ activity coefficient (calculated by PHREEQCi adopting the extended Debye–Hückel equation) and the free H^+ molality (Eq. (19), calculated using a spreadsheet) and computing the negative common logarithm of the resulting activity. This pH value was refined by repeating the PHREEQCi calculation and varying the input pH until the pH calculated from the PHREEQCi speciation was equal to the input pH. A flow-chart illustrating the process for refining the acidity pH is shown in Fig. 2.

4.5. Revised pH measurements

Accurate measurement of pH is of primary importance for interpretation of aqueous chemical speciation. Free H^+ is usually the major cation in samples with pH less than 2.5. In geothermal waters it is important in controlling geochemical reactions and is critical in calculating the charge imbalance (CI) for waters with pH < 3. For a subset of 108 samples with pH < 4.5, pH was determined using four different techniques: (1) pH measured in the field; (2) pH calculated from the acidity titration as described above; (3) pH measured at the USGS laboratory; and (4) pH calculated by adjusting the concentration of H^+ to yield a speciated CI of zero. Comparison of pH values from the 4 sources allows the

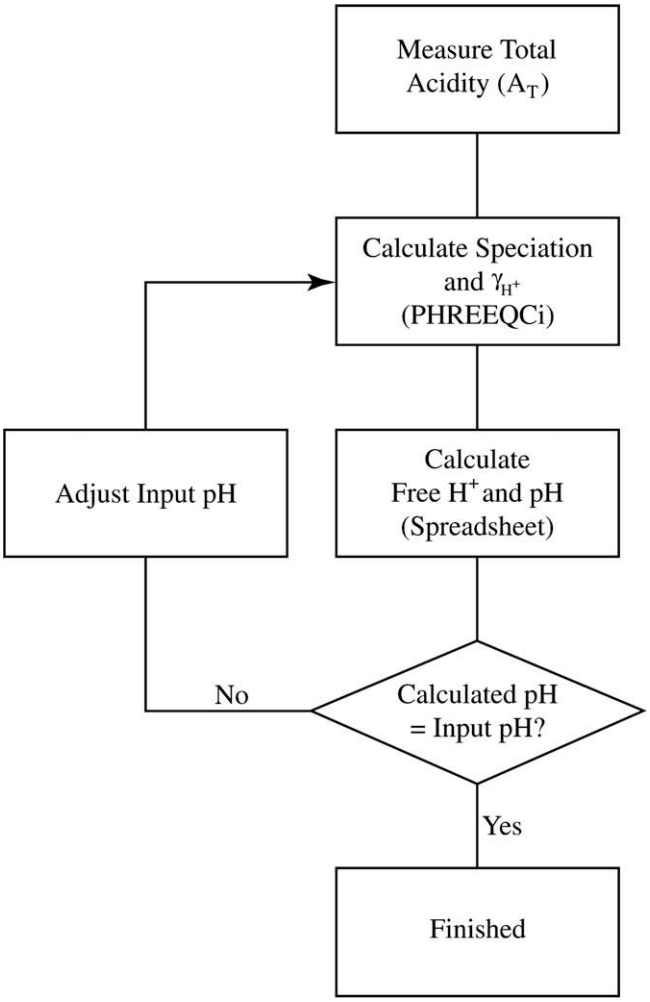

Fig. 2. Flow chart illustrating the process for refining the acidity pH value.

evaluation of the measurements and estimation of more accurate pH values.

A flow-chart showing the pH selection process is shown in Fig. 3. Field pH was considered to be the most accurate because pH measurements made in the laboratory may be biased from temperature changes or oxidation and hydrolysis reactions, and the acidity pH calculation relies on measurements of Fe, Al, SO_4, As, and F, all of which are subject to analytical uncertainties. Possible errors are related to the p*K* values of the considered reactions of hydrolysis and dissociation and to the model for calculating activity coefficients.

Field pH was selected for the final accepted pH for all samples with pH greater than 3.5. For samples having a pH less than 3.5, field pH was selected unless the sample had a speciated CI greater than 10%. For samples with pH less than 3.5 and speciated CI greater than 10% using field pH, acidity pH was selected if the speciated CI was less than 10%. Using the process described above and illustrated in Fig. 3, field pH was selected for 103 of 108 samples. The pH estimated from the acidity titration was used for the five samples with an apparent field pH measurement error. Table 3 shows examples of pH estimated by four different methods and their charge imbalance along with the final revised pH for the five samples with an apparent field pH measurement error. Table 3 also contains three other samples where there is excellent agreement between field pH and charge balance pH at field T and between acidity pH and charge balance pH at 22 °C.

5. Results and discussion

5.1. Changes in pH between field and laboratory

Positive differences between field and laboratory pH were found to be greatest for samples with field pH values between 4 and 6 and negative differences were greatest for samples in the pH range 5–8 (Fig. 4). Laboratory pH measurements typically are made at about 22 °C which can be as much as 72 °C less than the temperature at which the sample pH was measured. Differences in pH values between field and laboratory measurements are a function of the amount of Fe oxidized, the amount of reduced S oxidized, the amount of CO_2 and the change in sample temperature. Many of the samples that had pH reductions from field to laboratory were most likely poorly buffered, whereas samples that had

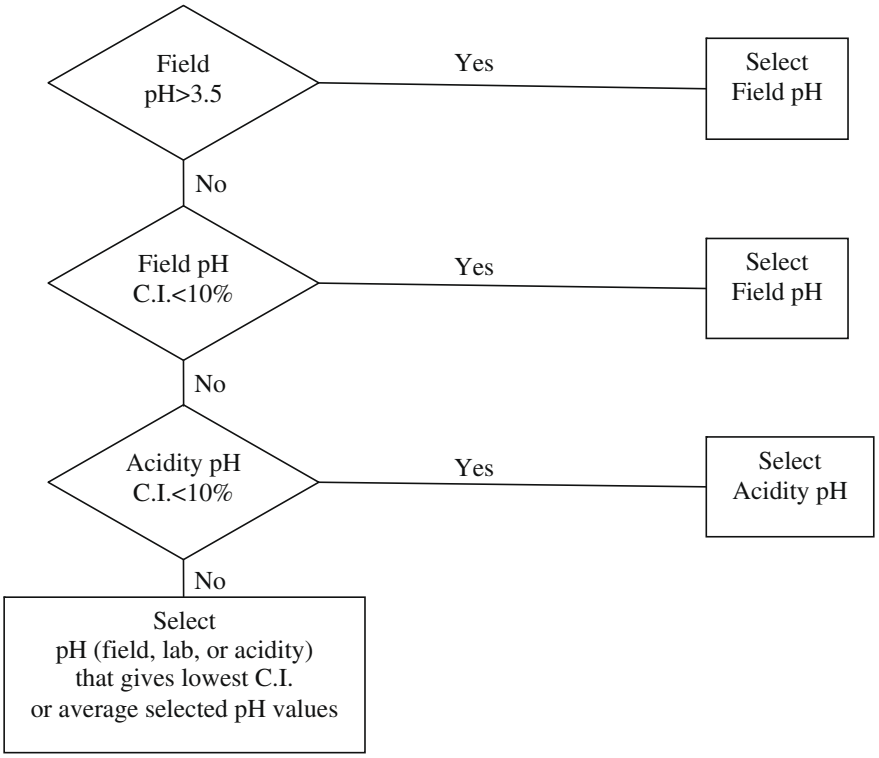

Fig. 3. Flow chart showing the pH selection process. CI = charge imbalance.

Table 3
Comparison of pH estimated by four methods for eight acidic samples. Temperatures in parentheses were not measured and were estimated.

Sample code	98WA133	97WA129	99WA117	99WA138	99WA140	03WA131	99WA124	04WA114
Temperature (°C)	13.5	18	18	(14)	(14)	74.3	91.5	81.3
Field pH	1.37	1.46	1.98	2.54	2.66	1.68	2.40	2.40
% CI	−34.5	−17.1	11.2	12.2	14.2	0.5	0.9	−1.3
Acidity pH at 22 °C	1.23	1.41	2.02	2.65	2.69	1.61	2.26	2.26
% CI	−0.2	−4.4	6.5	−1.5	8.4	−3.8	0.2	−0.7
Lab pH at 22 °C	1.26	1.53	2.06	2.76	2.85	1.52	2.30	2.32
% CI	−7.3	−31.7	1.7	−12.0	−15.0	15.4	−3.1	−9.9
Charge balance pH at 22 °C	1.22	1.39	2.07	2.64	2.75	1.59	2.26	2.26
Charge balance pH at field T	1.23	1.39	2.07	2.64	2.75	1.70	2.41	2.39
Revised pH	1.23	1.41	2.02	2.65	2.69	1.68	2.40	2.40

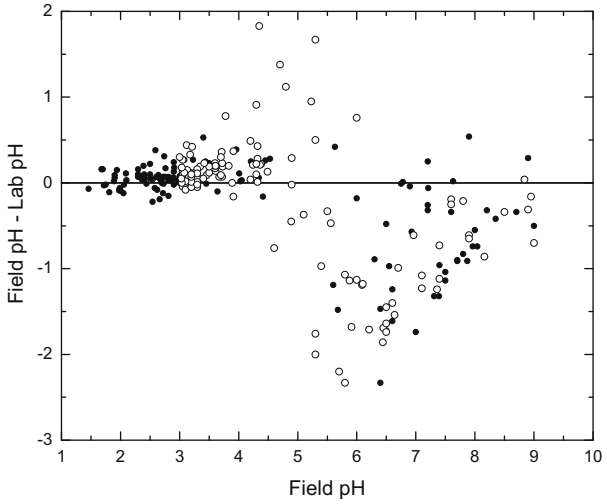

Fig. 4. Difference between field and laboratory pH as a function of field pH. Open circles indicate samples with pH > 3.2, and/or with Fe, H_2S, and S_2O_3 concentrations high enough to decrease the pH on oxidation.

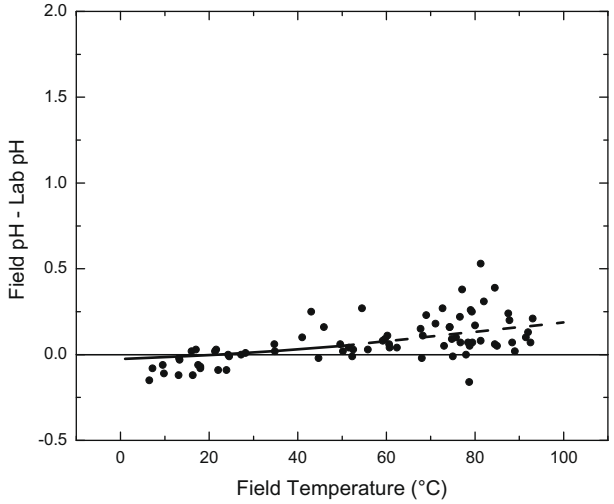

Fig. 5. Difference between field and lab pH plotted against field temperature, excluding samples with pH > 4.5 and samples with Fe, H_2S, and/or S_2O_3 > 0.5 mg/L. Sub-horizontal solid line represents pure sulfuric acid at a pH of 2.0 at 22 °C with a linear extrapolation (dashed) beyond the limits of temperature measured by Clegg et al. (1994).

pH increases were initially supersaturated with respect to atmospheric CO_2 and degassed.

As an example of how thiosulfate oxidation can affect the water chemistry, a sample from Cistern Spring was chosen with 17.7 mg/L thiosulfate at a pH of 5.29 and a SO_4 concentration of 72 mg/L. Several weeks later its pH had changed to 3.62. Thiosulfate oxidizes to H_2SO_4 according to the reaction

$$S_2O_3^{2-} + 2O_2 + H_2O \cdot 2H^+ + 2SO_4^{2-} \quad (21)$$

If the thiosulfate is fully oxidized, the final calculated pH should be about 3.63, nearly identical to the measured value. Further, it would have produced about 30 mg/L of SO_4. This result gives an incorrect SO_4 determination and could give an incorrect charge imbalance if H^+ is not included. If the thiosulfate is high enough, the charge imbalance also could be affected if thiosulfate is not in the calculation. This example shows how SO_4 determinations can yield values that are too high and variable depending on the concentration of thiosulfate in the original sample and how quickly it oxidizes before the SO_4 determination can be performed. This example also suggests that SO_4 determinations should be done promptly if thiosulfate is known to be present and SO_4 concentrations are low.

Water samples with enough reduced Fe or reduced S concentrations to cause a lowering of pH on oxidation are distinguished by open circles in Fig. 4. Calculations that estimate the pH change from the amount of reduced Fe and reduced S oxidized are reasonably close to the measured values for most samples shown above the line in Fig. 4. After eliminating changes caused by degassing or Fe and reduced S oxidation, there are still larger than expected variations between field and lab pH. Suspecting that the temperature change plays a role, a plot of this same difference (field pH–lab pH) as a function of temperature was made for just the low pH samples (Fig. 5). A distinct trend of increasing difference in pH with increasing temperature can be observed. On this plot, the line is drawn for pure H_2SO_4 having a pH of 2.0 at 22 °C and then drawn as a function of temperature while keeping constant the molal concentration using the Aerosol Inorganics Model (AIM, from Wexler and Clegg, 2002; http://www.aim.env.uea.ac.uk/aim/aim.php). The basic data are from Clegg et al. (1994). The trend in the cluster of data points follows the trend line which is caused by the temperature-dependence of pK_2, the second hydrolysis constant for H_2SO_4. The remaining variations in the data are likely caused by inaccurate field measurements and inaccuracies in automatic temperature compensators.

5.2. Charge balance/imbalance

Several techniques were used to assure the quality of the analytical data. These techniques included calculation of charge imbalance, CI, analysis of USGS standard reference water samples (SRWS), replicate analyses, spike recovery determinations, and determination by alternative analytical methods (Ball et al., 2007).

The charge-balance calculation is one of the first and simplest of quality assurance/quality control (QA/QC) procedures to check the accuracy of a water analysis. It is based on the principle

$$\sum_i c_i = 0 = \sum_i c_i^+ - \sum_i c_i^- \quad (22)$$

where c_i = the equivalent concentration (usually in milliequivalents/L) for the ith ion, C_i^+ = the equivalent concentration for the ith cation, and C_i^- = the equivalent concentration for the ith anion. The charge-balance calculation normally is obtained as a percentage by taking the difference of the equivalent concentration of cations and anions and dividing by the sum times 100

$$\frac{\sum_i^n c_i^+ - \sum_i^m c_i^-}{\sum_i^n c_i^+ + \sum_i^m c_i^-} \times 100 \quad (23)$$

where C_i^+ and C_i^- have the same meanings as above and n and m are the number of cations and anions in the solution, respectively.

The charge balance should be a quotient in which the divisor is the average of the sum of cation and anion equivalents, not just the sum (DVWK, 1990; Ball and Nordstrom, 1991; Hölting, 1996). The code WATEQ4F uses the average for the divisor as shown in Eq. (24) to calculate charge balance and to differentiate it, it is called the charge imbalance, CI

$$\text{CI } (\%) = \frac{\sum_i^n c_i^+ - \sum_i^m c_i^-}{(\sum_i^n c_i^+ + \sum_i^m c_i^-)/2} \times 100 \quad (24)$$

A frequency plot of CI for 709 samples is shown in Fig. 6. The Gaussian fit CI mean is −1.8% and the median is nearly the same, −2.0%, with 2 standard deviations of ±14%. Charge imbalances greater than ±20% were considered too unreliable for further interpretation and were excluded.

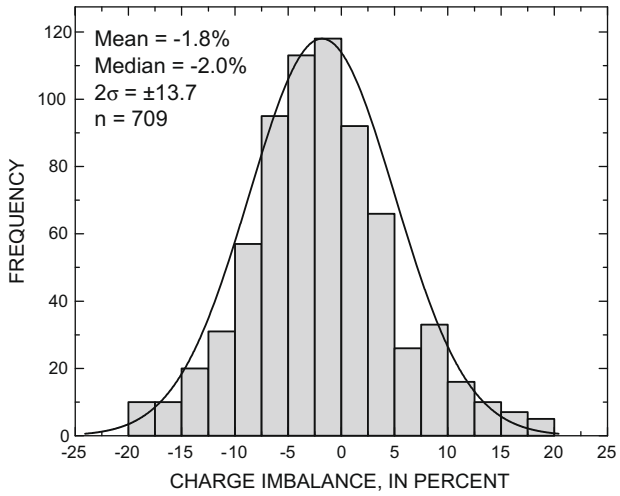

Fig. 6. Frequency of charge imbalance distribution for all Yellowstone samples having charge imbalance <±20%.

Two important errors in calculating charge imbalance arise for waters of low pH. One error has to do with omitting the H^+ concentration and the other has to do with omitting speciation.

Charge balances are routinely calculated by analytical laboratories using the major ions: Na, K, Ca, Mg, Cl, SO_4, HCO_3, ($\pm NO_3$, F). Usually, only one or two ions are a source of error in the charge balance. Once the pH drops below 3, the H^+ ion can become the major cation (about a milliequivalent). If the H^+ concentration is absent from the charge-balance calculation (which often happens), the charge balance will become progressively worse as the pH decreases. An example of charge imbalance calculated for acid–sulfate water samples without the inclusion of the H^+ ion is shown in Fig. 7A.

Omission or inclusion of the H^+ ion is not the only issue. In the charge balance computation, a charge of -2 is routinely attributed to total SO_4 concentration, which includes SO_4^{2-} and HSO_4^- ions. Considering that the pK of reaction (3) is 1.98, SO_4^{2-} is dominant (more than 85%) for pH > 2.7, where it is correct to attribute the charge of -2 to total SO_4 concentration. In contrast, the charge of -1 must be assigned to total SO_4 concentration below pH 1.3, where HSO_4^- prevails. In the pH range from 1.3 to 2.7, speciation calculations are mandatory to distribute total SO_4 concentration between SO_4^{2-} and HSO_4^{2-} ions.

Thus, if equivalent H^+ concentrations are extracted from the pH measurement (a measurement of H^+ activity, not concentration), the water must be speciated before charge balance can be calculated. All reactions shown in Eqs. (3)–(13) should be considered. Hence, charge balance is model-dependent for acid waters. Fig. 7B shows the divergence of analytical charge imbalance (unspeciated) from speciated charge imbalance (Fig. 7C) for acid samples, relative to the selected pH. Note that the divergence becomes significant (greater than a difference of 10%) when the pH is less than 3. The speciated charge imbalance shows no systematic bias as a function of pH.

5.3. Acidity titration pH and other measures of pH

The acidity titration, as mentioned earlier, gives an estimate of free H^+ concentration but at laboratory temperatures. Therefore, it should be directly compared to the laboratory pH measurement, not the field pH measurement. This comparison is made in Fig. 8. The values show a good fit up to about 2.7 in pH and then there is an increasing dispersion of the values. The variation between laboratory pH and acidity pH is a measure of the accuracy of pH

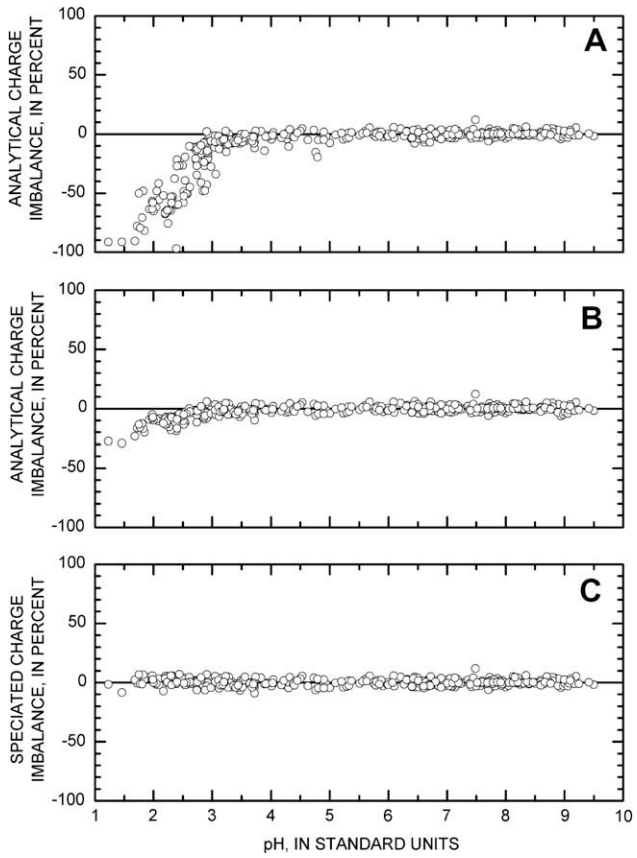

Fig. 7. (A) Charge imbalance calculated without any H^+. (B) Charge imbalance calculated with H^+ but without speciation. (C) Charge imbalance calculated with H^+ and speciation.

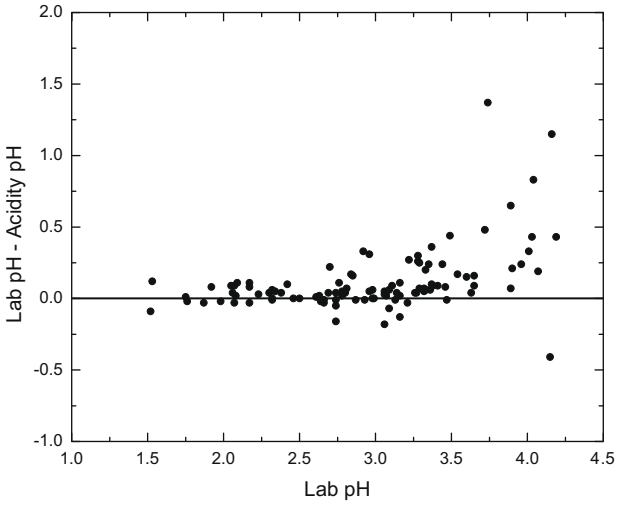

Fig. 8. Difference between lab pH and acidity pH plotted against lab pH.

measurements made under optimal (non-field) conditions. With pH values >2.7, the relative error in the acidity titration increases because the acidity is approaching the detection limit.

5.4. Distribution of pH values, sulfate concentrations, and water-chemistry types

As has been noted previously by Brock (1971, 1978), the pH of thermal waters worldwide has a bimodal distribution. Values that

have been carefully measured for 709 thermal features of Yellowstone National Park have a similar bimodal distribution (Fig. 9). This trend defines the first two categories of water types at Yellowstone: acidic (pH 1–5) or near neutral to basic (5–10). Marini et al. (2003) also reported a bimodal pH distribution for volcanic lake waters but their modes were notably lower than the present ones.

Although Brock (1971, 1978) has called these acid–sulfate waters and neutral-carbonate waters, it makes more sense to use the classification of White (1957) and call these acid–sulfate and neutral-chloride waters. To increase the database and include a wider range of Yellowstone thermal water chemistries, data from Thompson and DeMonge (1996) have been included.

Comparison of the acid–sulfate waters to pure H_2SO_4 in terms of pH and SO_4 concentrations (Fig. 10) demonstrates that when pH values fall below 3, the SO_4 concentration increases substantially and closely approximates the line for pure H_2SO_4. This trend occurs because, unlike acid mine waters, metal concentrations are comparatively low in thermal waters and H^+ is the dominant cation. In acid mine waters, Fe and Al dominate the cation concentrations at pH < 3 (Plumlee et al., 1999).

As the pH decreases below 3 the H^+ becomes an increasing percentage of the cation milliequivalents and for pH values below about 2.2, H^+ becomes more than 50 mol% of the total cations in mole percent (Fig. 11). This result contrasts substantially with acid rock drainage in which the H^+ concentration almost never exceeds 50 mol% of the cations.

The other noticeable trend in Fig. 10 is that at pH values greater than 3, average SO_4 concentrations decrease consistently with an increase of pH. At the highest pH values, typical of those found in the Upper, Midway, and Lower Geyser Basins, the SO_4 concentrations tend to range from 10 to 100 mg/L. Unfortunately the variance in the data is quite large. Much of the variance arises from the Thompson and DeMonge (1996) data and there were known difficulties with those determinations (Fournier and Thompson, oral communication, 2005). An example of SO_4 and Cl concentrations from Cistern Spring shown in Fig. 12 reflects this problem. The SO_4 and Cl concentrations from the present authors' determinations and those of Fournier et al. (2002); all by ion chromatography) show less variance than the Thompson and DeMonge (1996) data for the same spring.

Assuming that these problems with SO_4 determinations were worst for the low concentration data, Fig. 10 was replotted (Fig. 13) excluding the low SO_4 concentrations from Thompson's

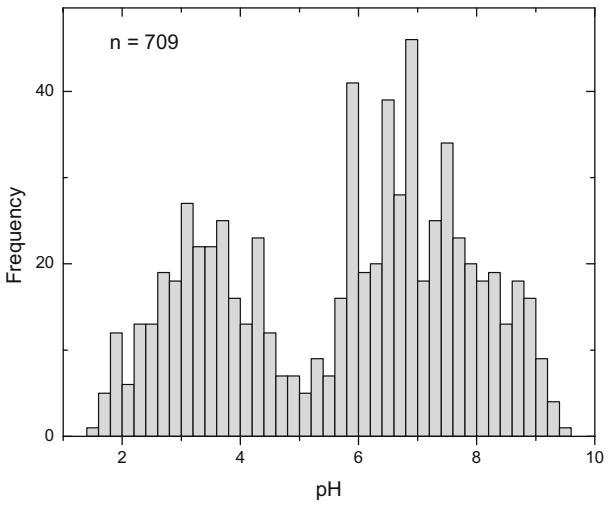

Fig. 9. Frequency distribution of pH for 709 samples of Yellowstone thermal waters.

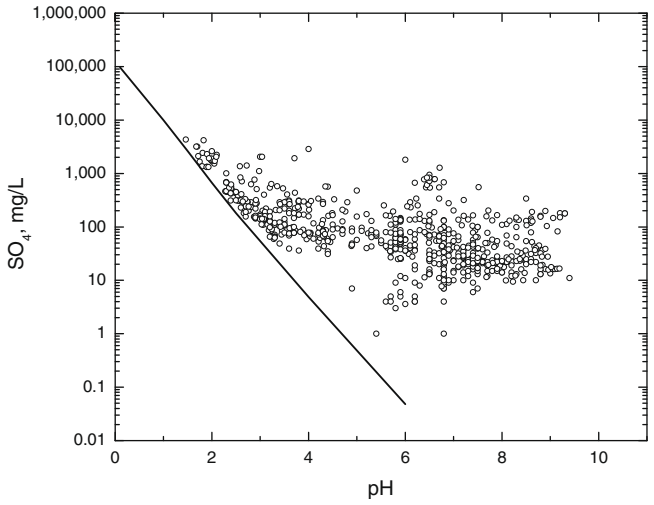

Fig. 10. Sulfate concentrations relative to pH for Yellowstone waters. Line shows relationship between these parameters for pure H_2SO_4 at 25 °C.

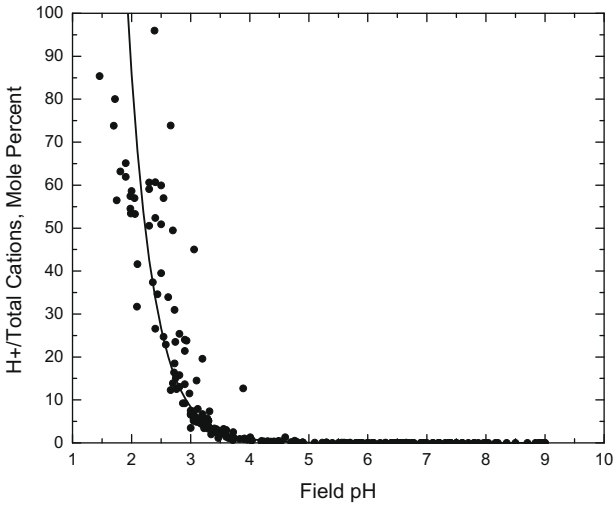

Fig. 11. Mole percent of H^+ of the total cations relative to field pH. At pH < 3 the H^+ concentration is substantial and at pH < 2.2 it is more than half of the cation concentration.

data, excluding samples with less than 350 mg/L Cl, excluding SO_4 concentrations greater than 500 mg SO_4/L, that would imply mixing with near-surface acid–sulfate waters, and excluding samples from the Mammoth Hot Springs area. Now the cluster of concentrations between 10 and 100 mg/L is more apparent. The mean for this dataset is 98 mg SO_4/L and the median is 73 mg SO_4/L. This trend may reflect the SO_4 concentration of the deep geothermal reservoir. If this hypothesis is true, it has important implications for deciphering the processes governing the SO_4 composition of Yellowstone thermal waters.

Neutral to basic waters are high in carbonate, silica, and chloride and were designated as type I waters by White et al. (1988) for Norris Geyser Basin. These waters were most closely associated with the original deep thermal water and reflect the highest temperature of origin. They also are typically devoid of ^3H and contain lighter stable water isotope compositions. Acid waters are further divided by White et al. (1988) into two more types: acid–sulfate waters (or White's type IV) and acid SO_4–Cl or Cl–SO_4 waters (or White's type III). White's type II were dilute meteoric waters, sometimes acidified (type IIb). The authors prefer to use a similar

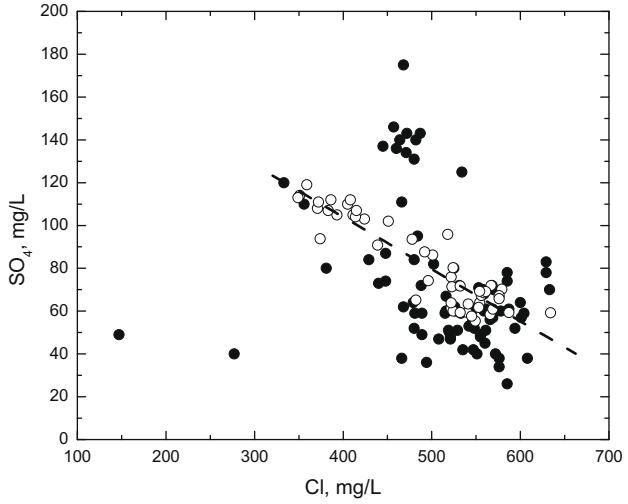

Fig. 12. Sulfate concentrations plotted against chloride concentrations for data from Cistern Spring. Filled circles are data from Thompson and DeMonge (1996). Open circles are from Ball et al. (2001, 2007), McCleskey et al. (2005) and Fournier et al. (2002). The dashed line is the best fit through the open circles.

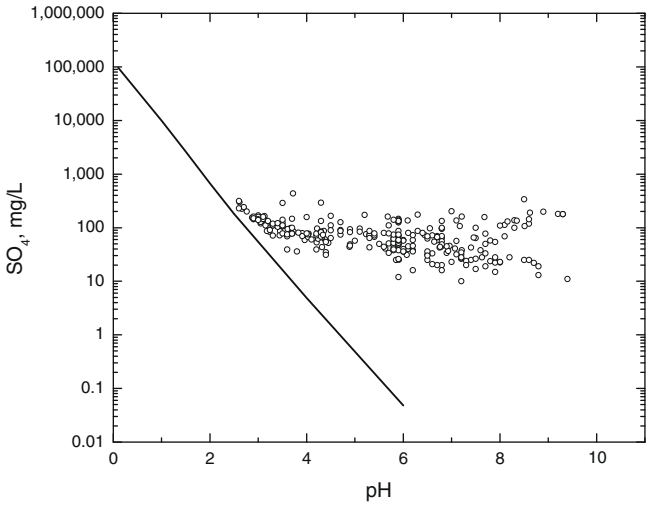

Fig. 13. Plot of SO_4 concentrations relative to pH excluding all samples with Cl concentration less than 350 mg/L, excluding Thompson and DeMonge's low SO_4 concentrations, excluding high SO_4 concentrations produced by mixing with near-surface acid–sulfate waters, and excluding Mammoth Hot Springs samples.

classification that can be applied to all waters in the Park in terms of the water source and processes influencing their chemistry. This classification also is based on trends in SO_4 and Cl concentrations and stable isotope compositions.

Dilute meteoric waters are one end-member fluid source and contain very low concentrations of SO_4 and Cl. These waters have seen little to no admixture of geothermal fluids (waters or gases). These will be referred to as meteoric only, MO. Some of these meteoric waters are impacted by geothermal gases only and have become acidic from H_2S oxidation. These will be called meteoric plus gas, MG. They are identified by low pH values, high SO_4 concentrations, and low Cl concentrations (generally less than 100 mg/L). Because SO_4 concentrations are highly variable, it can be confusing as a distinguishing variable. Sulfate concentrations >500 mg/L are typical of this MG group and SO_4 concentrations of 100–500 mg/L with Cl concentrations <100 mg/L are typical of this group. The large range in SO_4 concentration with low Cl concentration can be achieved in two ways, either through continual evaporation in a surface environment with S oxidation (to varying degrees) or through mixing between a more concentrated acid–sulfate water and dilute-meteoric water. In Fig. 14, $\delta^{18}O$ for water has been plotted relative to dissolved SO_4 concentrations. This trend toward highly enriched $\delta^{18}O$ is indicative of surface evaporation which has been described by several authors (Sakai and Matsubaya, 1977; Giggenbach, 1971, 1978, 1988; Truesdell and Huston, 1980; Panichi and Gonfiantini, 1981). Most of the acid high-SO_4 and low-Cl pools also have the heaviest $\delta^{18}O$ values and include the acid inkpot at Washburn, Sulphur Caldron (Mud Volcano area), Turbulent Pool (next to Sulphur Caldron), Evening Primrose (Gibbon Geyser Basin), Frying Pan Spring (Norris Geyser Basin), and Sylvan Springs (Gibbon Geyser Basin).

These high-SO_4, high $\delta^{18}O$ waters have been plotted in Fig. 15 for δD relative to $\delta^{18}O$ to show how they are the end-members of a linear correlation of values that have undergone boiling or near-boiling surface evaporation. The best fit slope of the correlation is close to 3, the same value that Craig (1963) and Giggenbach (1978) reported for heated surface evaporation occurring under non-equilibrium conditions. A few lake waters have been plotted which lie along a lower-temperature evaporation trend with a slope of about five. The intercept for the high-temperature correlation with the δD of the estimated meteoric recharge water is about −18.5‰ in $\delta^{18}O$ which is only 1.5‰ enriched from meteoric. This small $\delta^{18}O$ shift is indicative of a steady-state condition reached between the $\delta^{18}O$ of the recharging meteoric water, its flow velocity and the reacting rock with its $\delta^{18}O$ value. Other isotope data from Yellowstone have suggested that the $\delta^{18}O$ shift caused by oxygen exchange with rock is more like 4‰. However, there are some data points from Josephs Coat Spring (open squares) that suggest meteoric recharge is a little different here and the $\delta^{18}O$ shift may be as much as 5‰. This location might be recharged with water of a different isotopic composition because of its location in the northeastern part of the Park, a different rock composition, more transient-state conditions, or all of the above.

Another end-member fluid source is the deep-seated hydrothermal water that has been estimated by Fournier (2006) to have a Cl concentration of about 310–400 mg/L. This source will be termed hydrothermal only, HO. This fluid can undergo three important processes on its way to the surface: adiabatic decom-

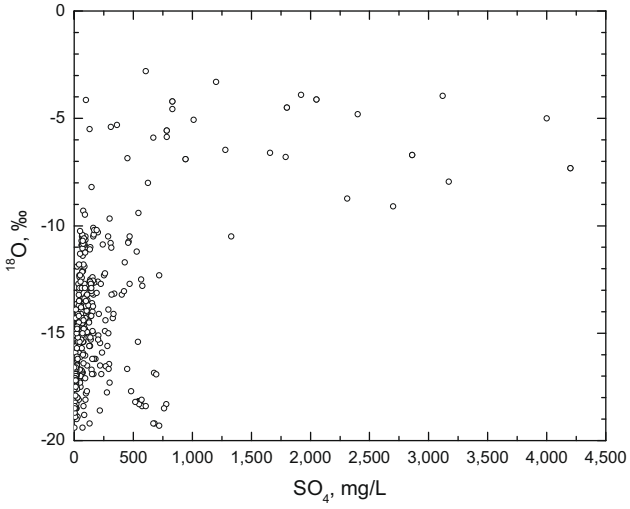

Fig. 14. Plot of $\delta^{18}O$ relative to SO_4 concentrations showing evaporative concentration of waters through hot gas discharge with variable SO_4 concentrations caused by varying amounts of S oxidation.

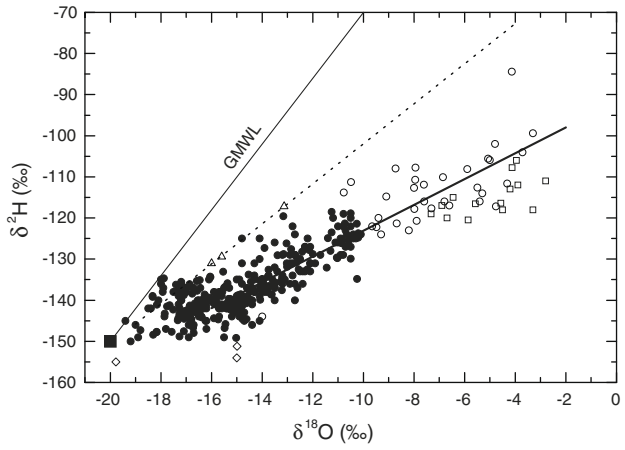

Fig. 15. Plot of δD against $\delta^{18}O$ to show the near-boiling evaporative trend of Yellowstone waters with the most enriched shown with open circles corresponding to those in Fig. 14 with SO_4 concentration greater than 1000 mg/L. GMWL = global meteoric water line, dotted line has slope of 5, similar to evaporating lakes, and solid bold line has slope of 3, typical of evaporating thermal waters. The solid square shows the average recharge water estimated by Kharaka et al. (2002) and Rye and Truesdell (1993). Open diamonds are from Josephs Coat Springs and Hot Spring Basin. Open squares are from Washburn Hot Springs. Open triangles are lake waters.

pression (boiling), mixing with acid–sulfate waters (MG) infiltrating from the surface, and mixing with dilute meteoric waters (MO). Boiling should increase solute concentrations unless mineral solubility or another equilibrium provides a constraint. Hydrothermal waters that have only undergone boiling will be termed HB. Mixing with acid–sulfate waters will increase SO_4 concentration but should decrease Cl concentrations. Mixed waters will be designated on the diagram with a double-headed arrow. These trends are displayed in Fig. 16.

5.5. Hydrothermal sulfate

Two end-member sources of low SO_4 concentration have been identified: MO and HO. The low SO_4 concentration of HO water (10–100 mg/L) is now better understood from recent studies that have applied more detailed geochemical and isotopic data. Kameda (1963) suggested that sulfates in thermal waters at Iwojima were produced by disproportionation of SO_2 in volcanic gases. Holland (1965) pointed out from thermodynamic calculations that in magmatic hydrothermal fluids (temperatures >400 °C), S should occur predominately as SO_2 and at lower temperatures the SO_2 should disproportionate. This idea has gained support from subsequent studies (Burnham and Ohmoto, 1980; Ohmoto and Goldhaber, 1997). As this fluid cools, a disproportionation reaction should take place to produce sulfide and sulfate

$$4SO_2 + 4H_2O = 3H_2SO_4 + H_2S \quad (25)$$

Currently, the lower temperature limit for disproportionation is thought to be closer to 300 °C (Einaudi et al., 2003). Further, as the fluid rises to the surface and is cooled, it is thought that the SO_4 is generated gradually over some temperature range (Rye, 1993). This development of SO_4 leads to acid–sulfate alteration at temperatures >90 °C. Such fluids can also mix with MG fluids infiltrating from surface environments (supergene conditions) making it difficult to distinguish supergene from hypogene acid–sulfate alteration. Under these hypogene conditions, sulfide and sulfate minerals also form. The mineral-solubility data summarized by Holland (1967) shows that anhydrite solubility decreases substantially at high temperatures compared to lower temperatures and equilibrium SO_4 concentrations below 100 mg/L are easily reached.

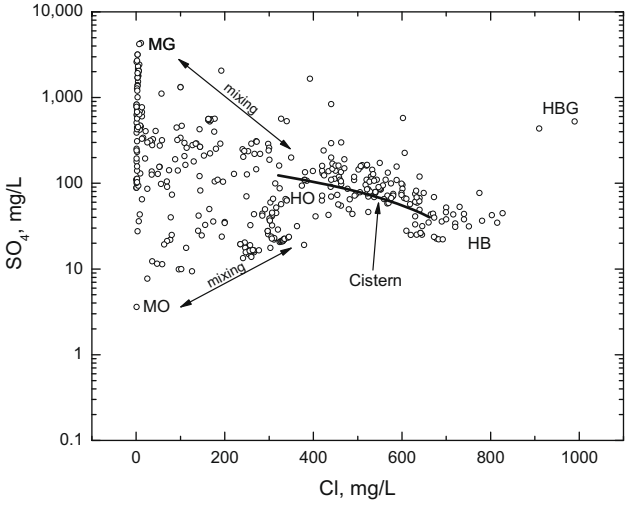

Fig. 16. Sulfate concentrations plotted relative to Cl concentrations for all Yellowstone waters except those from Thompson and DeMonge (1996). HO = hydrothermal only (deep reservoir source), HB = hydrothermal with subsurface boiling, MO = meteoric water only, MB = meteoric water with hot gas discharge, HBG = hydrothermal with subsurface boiling and hot gas discharge.

Table 4
Chemical compositions of the three acidic outflows from Norris Geyser Basin. Dashed line with no value means substance was not analyzed.

Sample location	Tantalus Creek at weir	Realgar Creek near mouth	Gap SW outflow
Date collected	9/14/2006	9/12/2006	5/15/2006
Discharge (CFS)	2.9	0.13	0.16
Temperature (°C)	23.6	28.2	36.8
pH (field/lab)	3.02/3.02	3.05/3.00	3.08/3.06
Spec. cond. (μS/cm)	2290	2330	1815
Eh (V)	–	0.702	0.694
Density (g/mL at 20 °C)	0.9993	0.9993	0.9991
Constituent (mg/L)			
Ca	4.09	4.58	3.53
Mg	0.231	0.21	0.381
Na	310	310	254
K	56.3	50.1	28.3
SO_4	160	157	119
F	5.26	5.74	4.99
Cl	515	524	379
Br	2.03	1.63	1.24
NO_3	0.10	<0.05	0.08
NH_4	1.40	1.29	0.93
SiO_2	364	261	302
Al	2.47	3.59	2.52
Fe(T)	1.27	1.10	3.04
Fe(II)	0.203	0.296	1.23
B	7.63	8.06	5.49
Li	3.93	2.72	2.09
Sr	0.016	0.025	0.015
Ba	0.083	0.111	0.118
Mn	0.08	0.037	0.077
Zn	0.018	0.009	0.016
Pb	<0.008	<0.008	<0.008
As(T)	1.50	1.30	0.837
As(III)	0.029	0.035	0.049
Sb(T)	0.032	0.036	0.010
Sb(III)	<0.0005	0.0007	<0.0005
Mo	0.048	<0.007	<0.007
Hg (ng/L)	17	22	26
Methylmercury (ng/L)	0.04	0.05	–
DOC (mg/L)	1.2	0.79	0.9
Deuterium (‰)	−132	−132	−139
O-18 (‰)	−13.0	−13.3	−14.8

Table 5
Chemical analyses of Crystal Spring in Norris Geyser Basin, 2002–2007. Dashed line with no value means substance was not analyzed.

Sample location	Crystal Spring	Crystal Spring	Crystal Spring western side	Crystal Spring eastern side	Crystal Spring western side	Crystal Spring eastern side
Date collected	6/28/2002	6/7/2005	5/13/2006	5/13/2006	9/18/2007	9/18/2007
Temperature (°C)	83.7	82.0	80.3	80.6	82.9	77.0
pH (field/lab)	6.00/7.13	5.33/4.83	3.77/3.67	5.55/6.25	1.98/1.94	1.97/1.96
Spec. cond. (μS/cm)	2230	2200	2360	2320	3380	3660
Eh (V)	−0.035	0.084	0.143	0.047	0.180	0.500
Density (g/mL at 20 °C)	0.9995	0.9994	0.9994	0.9994	0.9996	0.9995
Constituent (mg/L)						
Ca	6.22	6.16	6.08	6.52	1.88	2.17
Mg	0.009	0.010	<0.007	<0.007	0.212	0.212
Na	426	420	429	448	83.8	95.8
K	33.9	34.4	30.5	31.4	11.7	13.0
SO_4	35.8	43.2	52.6	31.0	1267	1185
S_2O_3	3.0	1.8	1.63	2.26	<0.1	<0.1
H_2S	0.10	0.085	0.09	0.14	<0.002	<0.002
Total alkalinity (as HCO_3)	14.4	<1	–	6.07	–	–
F	6.84	6.60	7.29	6.73	2.43	2.56
Cl	690	716	708	722	108	145
Br	2.28	2.20	2.36	2.95	0.470	0.491
NO_3	<0.1	0.022	<0.05	<0.05	0.087	0.085
NH_4	1.35	1.00	1.39	1.19	11.4	11.5
SiO_2	430	453	385	418	228	259
Al	0.199	0.382	0.670	0.240	22.8	25.7
Fe(T)	0.035	0.072	0.034	0.02	3.10	4.23
Fe(II)	0.033	0.068	0.034	0.019	2.94	2.01
B	10.9	10.4	9.78	10.2	1.90	2.37
Li	5.56	5.66	4.74	4.92	0.82	1.04
Sr	0.013	0.012	0.013	0.014	0.010	0.010
Ba	0.007	0.007	0.009	0.007	0.054	0.058
Mn	0.002	0.005	0.004	0.004	0.037	0.040
Zn	<0.001	0.001	<0.004	<0.004	0.015	0.012
Pb	0.0009	0.0025	<0.008	<0.008	<0.008	<0.008
As(T)	2.90	2.69	2.46	2.47	0.686	0.610
As(III)	2.88	2.45	2.46	2.39	0.498	0.074
Sb(T)	0.149	0.132	0.126	0.132	0.126	0.144
Sb(III)	–	0.057	0.126	0.124	–	–
Mo	0.219	0.213	0.203	0.209	0.072	0.127
Hg (ng/L)	52	53	97	139	470	270
DOC (mg/L)	–	0.6	0.6	0.4	3.76	2.86
Deuterium (‰)	−139	−137	−132	−135	−117	−116
O-18 (‰)	−14.1	−13.5	−11.0	−12.9	−7.6	−6.3

Under experimental conditions, Mottl and Holland (1978) showed that when seawater reacts with basalt at 200–500 °C, anhydrite is formed throughout the temperature range. Basalt–seawater reactions in the laboratory at 300 °C reported by Seyfried and Bischoff (1981) also showed large depletions in SO_4 from anhydrite precipitation and the final SO_4 concentrations were 20–80 mg/L. Increasing the ionic strength increases anhydrite solubility but NaCl concentrations in Yellowstone thermal waters are not extremely high (highest Cl is about 1000 mg/L). Although aqueous sulfide and sulfate concentrations are predicted to increase with decreasing temperatures, mineral precipitation (anhydrite and sulfide minerals) tends to keep these concentrations low and somewhat constant.

Empirical data indicate SO_4 concentrations in deep geothermal fluids are typically low. Ellis and Mahon (1977) state that SO_4 concentrations are somewhat erratic but rarely greater than 100 ppm and that the higher the temperature of the fluid, the lower the SO_4 concentration. Giggenbach (1997) lists SO_4 concentrations of <5–105 mg/L for high-temperature fluids with pH between 6.5 and 8.5 (neutral-chloride thermal waters) suggesting that removal of sulfate by mineral precipitation would account for the low concentrations. Arnórsson et al. (1978) lists SO_4 concentrations of 28–122 mg/L for four high-temperature geothermal systems in Iceland and additional analyses in Arnórsson (1995) range from 3.67 to 166 mg/L. Mariner et al. (1993) provided strong evidence for anhydrite solubility equilibrium in geothermal waters of the Cascades and Modoc Plateau and indicated it could be used as a geothermometer. In shallow hot springs, alunite could also provide a solubility constraint (Raymahashay, 1968; Stoffregen et al., 2000).

Ellis and Mahon (1977) estimated that about 15 ppm SO_4 would form from the quantitative oxidation of sulfide by oxygenated meteoric water for New Zealand thermal waters. Truesdell et al. (1978) showed that there was a distinct lower limit to SO_4 concentrations in Yellowstone thermal waters. They did a calculation similar to that of Ellis and Mahon (1977) and postulated that a SO_4 concentration of 13 ppm could be produced by reaction of atmospheric O_2 with sulfide. With further transport to the surface this water would boil to various degrees to produce higher concentrations. If this process predominated then the data should show SO_4 and Cl increasing concurrently at high concentrations. Fig. 16 shows this plot for the authors' Yellowstone data with a plot of the correlated data for Cistern Spring (Norris Geyser Basin) shown as a solid line. The trend appears to be the reverse. Sulfate decreases with increases in Cl. This trend can be explained either by mixing, by a mineral-solubility control such as anhydrite solubility that decreases with increasing temperature, or by boiling off of H_2S during steam separation and re-equilibration of the sulfide–sulfate speciation to give lower SO_4 concentrations. This last mechanism also would result in lower SO_4 concentrations with

Table 6
Chemical analyses of Frying Pan Spring, 1994–2005. Dashed line with no value means substance was not analyzed.

Sample ID	Frying Pan Spring	Frying Pan Spring	Frying Pan Spring
Date collected	6/29/1994	8/13/1997	6/8/2005
Temperature (°C)	78.2	60.6	60.7
pH (field/lab)	2.34/2.42	2.22/2.58	2.42/2.38
Spec. cond. (μS/cm)	1230	1450	1480
Eh (V)	0.182	0.369	0.228
Density (g/mL at 20 °C)	0.99889	0.9988	0.9988
Constituent (mg/L)			
Ca	2.41	2.29	2.51
Mg	0.530	0.38	0.539
Na	54.6	61.2	44.4
K	13.0	14.6	10.4
SO_4	437	362	422
S_2O_3	0.632	–	<0.1
H_2S	1.03	0.02	<0.001
F	2.95	3.43	1.90
Cl	8.69	12.1	7.90
Br	<0.04	<0.04	0.100
NO_3	<0.031	<0.2	0.020
NH_4	1.16	–	0.81
SiO_2	221	179	178
Al	5.65	4.14	12.3
Fe(T)	1.09	1.43	1.12
Fe(II)	1.09	1.41	1.02
B	0.64	1.50	0.44
Li	0.31	0.418	0.323
Sr	0.014	0.011	0.018
Ba	<0.06	0.058	0.054
Mn	<0.12	0.015	0.035
Zn	0.108	<0.004	0.007
Pb	<0.15	0.002	<0.0008
As(T)	0.19	0.287	0.150
As(III)	–	–	0.142
Sb(T)	–	–	0.0127
Sb(III)	–	–	0.009
Mo	–	–	<0.007
Hg (ng/L)	–	–	57
DOC (mg/L)	1.8	–	2.3
Deuterium (‰)	−123	−119	−126
O-18 (‰)	−11.9	−10.8	−13.0

Table 7
Chemical analyses of three acid pools in the Mud Volcano area. Dashed line with no value means substance was not analyzed.

Sample location	Sulphur Caldron	Turbulent Pool	Mud Geyser
Date collected	6/5/2003	9/11/2007	6/5/2003
Temperature (°C)	74.3	59.3	34.7
pH (field/lab)	1.68/1.52	1.99/2.00	1.93/1.87
Spec. cond. (μS/cm)	6800	3660	5350
Eh (V)	0.48	0.017	0.42
Density (g/mL at 20 °C)	1.0017	0.9996	1.0000
Constituent (mg/L)			
Ca	61.8	13.1	45.2
Mg	14.0	5.94	21.9
Na	20.3	15.5	73.1
K	22.9	11.2	26.4
SO_4	3170	1370	1330
H_2S	<0.002	<0.002	<0.002
F	1.00	0.980	0.400
Cl	2.72	7.36	100
Br	0.102	<0.03	0.370
NO_3	0.279	<0.05	<0.1
NH4	0.89	11.1	4.51
SiO_2	456	249	247
Al	122	41.7	40.3
Fe(T)	24.8	20	21.1
Fe(II)	24.6	20	15.0
B	3.58	0.85	2.10
Li	0.037	0.012	0.040
Sr	0.211	0.139	0.352
Ba	0.073	0.055	0.044
Mn	0.869	0.376	1.50
Zn	0.247	0.097	0.058
Pb	0.022	0.012	0.0016
As(T)	0.003	0.001	0.017
As(III)	0.003	0.001	0.012
Sb(T)	0.0020	0.036	0.0020
Mo	<0.007	<0.007	<0.007
Hg (ng/L)	120	39	22
Methylmercury (ng/L)	6.69	5.82	–
DOC (mg/L)	8.1	6.13	4.3
Deuterium (‰)	−108	−102	−111
O-18 (‰)	−7.9	−7.6	−10.5

more (or higher temperature) boiling consistent with the trend in Fig. 16. The Cistern Spring trend is reported to be a result of mixing (Fournier et al., 1986) but in this instance the high-Cl end-member must have low SO_4 concentration which requires either mineral precipitation or degassing. These three processes: mineral solubility, degassing and mixing, all have to be considered when interpreting the low SO_4 concentrations of these thermal waters.

Some of these waters must have undergone surface evaporation after boiling at depth such that the gas coming up with fluid adds some SO_4 from S oxidation to an already Cl-enriched fluid. This composition is called HBG (hydrothermal boiling followed by gas discharge with surface oxidation of S) and the best example is Sulphur Spring in Crater Hills (north of Mud Volcano area), the two data points that have 900–1000 mg/L Cl in Fig. 16.

5.6. Norris Geyser Basin acid waters

Norris Geyser Basin has a large number of acid waters. The basin has only three known outflows all of which drain into the Gibbon River. Analyses from these outflows, Tantalus Creek, Realgar Creek and the Gap outflow (to the west) are shown in Table 4. These waters are near pH 3 and contain high concentrations of SiO_2, Na, Al, Fe, Cl, SO_4, F, B, NH_4, and Li. These flows are small compared to the Gibbon River and have only a barely detectable effect on buffering capacity. Above the point of the first confluence, the Gibbon River has a pH of 6.88 and below the last confluence point it is 6.83 for September 12, 2006. The alkalinity is more detectable decreasing from 43.6 to 38.2 mg HCO_3/L. On September 20, 2005 there was virtually no change in pH or alkalinity in the Gibbon River from above to below Norris Geyser Basin outflows. Much more noticeable is the increase in concentration and loading of Cl, SO_4, SiO_2, F, and As for the Gibbon River (McCleskey et al., written communication, 2007).

Norris has some of the most As-rich waters in Yellowstone. Concentrations are typically 1–2 mg/L in several of the hot springs in the Gap and One Hundred Spring Plain. The highest As concentration found in this area is 9 mg/L in a new hydrothermal discharge in the Gap sampled on September 13, 2001.

One unusual process observed infrequently at Norris Geyser Basin with repeated monitoring is the complete change in water chemistry from a neutral-chloride water to an acid–sulfate water. One of the best examples is Crystal Spring, at the northern edge of Ragged Hills and the southwestern edge of One Hundred Spring Plain. Over the course of only one year the eastern discharge point changed from a circumneutral pH spring to a highly acid, highly evaporated, Hg-enriched and As-depleted spring. There is no known surface water source of highly evaporated water with such high SO_4 concentrations that could have mixed into this spring to change its composition. It appears that hot, evaporated groundwaters near the water table moved into this spring. A time sequence of analyses from this spring is shown in Table 5.

One of the best examples of MG-type water is Frying Pan Spring which drains into Nymph Lake at the northern end of Norris Geyser Basin. It has low Cl concentrations and provides one of the best

Table 8
Chemical analyses of inkpots at Washburn Hot Springs. Dashed line with no value means substance was not analyzed.

Sample location	Inkpot #1	Inkpot #2	Inkpot #3
Date collected	6/3/2003	6/3/2003	6/3/2003
Temperature (°C)	82.9	84.5	69.0
pH (field/lab)	6.45/8.09	6.61/8.01	3.04/2.74
Spec. cond. (μS/cm)	2135	2050	4460
Eh (V)	−0.178	−0.168	0.083
Density (g/mL at 20 °C)	0.9994	0.9995	1.0005
Constituent (mg/L)			
Ca	22.2	22.6	38.4
Mg	9.76	10.1	18.9
Na	34.7	35.0	29.8
K	11.1	11.3	14.2
SO_4	830	783	2050
H_2S	2.3	1.0	4.6
Total alkalinity (as HCO_3)	168	145	–
F	0.500	0.500	0.400
Cl	0.86	0.82	5.81
Br	0.1	0.1	0.1
NO_3	<0.1	0.15	0.1
NH_4	281	263	571
SiO_2	178	152	233
Al	0.076	0.092	16.8
Fe(T)	<0.002	0.012	14.9
Fe(II)	<0.002	0.010	14.9
B	5.67	4.27	6.52
Li	0.019	0.018	0.040
Sr	0.142	0.144	0.201
Ba	0.064	0.062	0.031
Mn	0.124	0.141	0.712
Zn	<0.004	<0.004	0.081
Pb	<0.0008	<0.0008	<0.0008
As(T)	0.003	0.003	0.0004
As(III)	0.003	0.003	<0.001
Sb	0.0020	<0.001	<0.001
Sb(III)	–	–	–
Mo	<0.007	<0.007	<0.007
Hg (ng/L)	2100	510	83
Methylmercury (CH_3Hg), ng/L	0.194	–	–
DOC (mg/L)	17	21	–
Deuterium (‰)	−113	−117	−108
O-18 (‰)	−4.21	−5.57	−4.12

examples of sulfide-rich steam mixing with local meteoric water. Table 6 tabulates three examples of its water chemistry which does not change substantially from year to year.

5.7. Mud Volcano area

Within the Yellowstone caldera there is one large area of strongly acidic waters of the MG type, Mud Volcano. Among the most acidic pools are Sulphur Caldron, Turbulent Pool, and Mud Geyser (Table 7). Sulphur Caldron has the lowest pH and the highest methylmercury and Hg concentrations of any hot spring in the Park. This water is also unusual in that the K concentration is greater than the Na concentration and it is one of the most evaporated waters in the Park.

5.8. Washburn Hot Springs

There are four main pools, or inkpots, at Washburn Hot Springs. Three are circumneutral in pH and one is acid. Table 8 shows one analysis of the acid inkpot (#3) and two of the circumneutral pools at Washburn. One of the unusual characteristics of both neutral pH and acid waters at Washburn is that they all contain extraordinarily high concentrations of NH_4. The SO_4 concentrations are also much higher than other circumneutral pH waters in the Park. These are also among the most isotopically enriched waters in the Park.

Table 9
Three acid–sulfate waters typical of low-temperature oxidative weathering of S at Brimstone Basin. Dashed line with no value means substance was not analyzed.

Sample location	Small tributary to Alluvium Creek	Small tributary to Alluvium Creek	Alluvium Creek at mouth
Date collected	8/12/1997	9/18/1998	9/18/1999
Temperature (°C)	18.0	13.5	6.5
pH (field/lab)	1.46/1.53	1.37/1.26	2.81/2.96
Spec. cond. (μS/cm)	18,360	38,100	1469
Eh (V)	0.603	–	0.718
Density (g/mL at 20 °C)	1.001	1.003	0.9993
Constituent (mg/L)			
Ca	19.9	35	41.5
Mg	11.6	20	33.9
Na	35.5	48	18.0
K	44.8	57	9.00
SO_4	4320	6500	630
F	0.354	3.0	<0.25
Cl	10.7	21	1.50
SiO_2	96.7	110	97.8
Al	87.6	100	49.4
Fe(T)	14.5	25.2	2.39
Fe(II)	12.9	23.2	0.172
B	0.023	0.066	0.009
Li	0.018	0.030	0.018
Sr	0.382	0.68	0.584
Ba	0.018	0.016	0.010
Mn	0.375	0.670	0.673
Zn	0.054	0.091	0.040
Pb	0.003	<0.0001	0.011
Co	<0.007	0.031	0.016
Ni	0.181	<0.02	0.028
Cu	<0.00005	0.002	0.010
Cd	<0.00002	0.002	<0.005
As(T)	0.014	0.004	<0.0002
As(III)	–	<0.0005	<0.0003
Deuterium (‰)	−134	−125	−140
O-18 (‰)	−20.1	−20.3	−18.6

5.9. Brimstone Basin

Brimstone Basin is a large hydrothermally altered area in the southeastern part of the Park, adjacent to Yellowstone Lake. The Washburn expedition party of 1870 reported no thermal anomalies and Langford (1905) mentions "the volcanic activity in this vicinity is evidently decreasing." He also mentions "sulphur water" in numerous rivulets draining the mountainside. Indeed, Alluvium Creek is mostly composed of H_2SO_4 and tributaries of Columbine Creek contain H_2SO_4. These are the two main creeks that drain Brimstone Basin. The highly altered volcanic rocks in this area contain S and the tops of some of the hillsides have S lava flows. These are likely to have formed by ignition from hot cinders from a forest fire landing on elemental S. The S is weathering at low-temperature to H_2SO_4 which reaches pH values less than 2 in some locations. Three examples of low-pH waters in the basin are shown in Table 9. The 9/18/98 sample with pH of 1.23 is the lowest pH water the authors have found in the Park. Again, in contrast to acid rock drainage, the concentrations of Cu, Zn, Pb, and Cd are very low. Even Fe and Al concentrations are much lower than those in acid rock drainage.

Concentrations of elements indicative of thermal fluids such as B, Li, Cl, and As are notably low or below detection in these waters. There is nothing in the temperature measurements or in the water chemistry to indicate thermal activity. Some gases bubbling into the streams were observed in several places. Whether these gases are some late stage, spent thermal fluids escaping to the surface or shallow subsurface production of gases is unclear without some analyses. Some of these gases contained H_2S and others did not.

Preliminary data have shown, as expected, that the chemoautotrophic S-oxidizing bacterium *Acidithiobacillus thiooxidans* is dominant over Fe-oxidizing chemoautotrophic bacteria (Southam et al., 1997). The only visible form of life in these waters was fly larvae. These are described in the next section.

6. Eukaryotic life in acid–sulfate waters

Two genera of fly larvae have been found in acid–sulfate waters of pH 2–3 at Yellowstone National Park. These waters have some of the lowest pH values in which any eukaryote has been observed to live and successfully reproduce. The flies are in the Diptera Order of the Insecta Class. One of the genera of larvae was from the Stratiomyidae Family, commonly known as soldier flies and has been tentatively identified as related to *Odontomyia occidentalis* (G.G. Geesy, Montana State University, written communication, 2007). The unusual aspect of this larva was its aquatic habitat. It was surviving in a thermal water of about 30 °C, pH 2.87, and containing more than 5 mg/L dissolved As. The chemical analysis of this water is shown in Table 10. At the time of this observation, there were dozens of these fly larvae that were swimming upstream in several

Table 10
Three chemical analyses of waters in which fly larvae were found. The first is a small stream in Norris Geyser Basin near the Gap in which Straiomyidae were found and the other two are in Brimstone Basin in which Ephydridae were found. Dashed line with no value means substance was not analyzed.

Sample ID	Small side drainage near NRHANNI	Alluvium Creek ~ 2000 ft. upstream from Thorofare trail	Alluvium Creek at sulfur mounds
Date collected	6/23/2000	9/18/1999	9/18/1999
Temperature (°C)	29.8	18.0	17.5
pH (field/lab)	2.87/2.83	1.98/2.06	1.99/2.05
Spec. cond. (μS/cm)	2430	5740	6070
Eh (V)	–	0.732	0.656
Density (g/mL at 20 °C)	0.9993	1.000	1.001
Constituent (mg/L)			
Ca	5.7	82.7	83.7
Mg	0.30	93.6	95.2
Na	320	34.0	34.0
K	37	30.4	33.0
SO_4	140	1800	1900
S_2O_3	<0.1	–	–
H_2S	<0.001	–	–
F	2.6	0.26	0.29
Cl	530	3.68	3.88
Br	0.79	<0.1	<0.1
NO_3	<0.1	<0.4	<0.4
NH_4	0.44	–	–
SiO_2	310	90.0	85.4
Al	4.3	76.1	80.2
Fe(T)	2.96	15.2	14.7
Fe(II)	2.00	1.02	1.63
B	8.7	0.023	0.019
Li	3.2	0.041	0.043
Sr	0.015	0.992	1.02
Ba	0.13	0.010	0.012
Mn	0.042	1.52	1.57
Zn	0.010	0.056	0.055
Pb	0.002	0.015	0.018
As(T)	5.4	0.0005	0.0003
As(III)	0.28	<0.0003	<0.0003
Sb(T)	0.001	–	–
Deuterium (‰)	−139	−138	−139
O-18 (‰)	−14.6	−21.3	−21.9

Fig. 17. Photograph of Ephydrid fly larvae in about 3 cm of Alluvium Creek water with pH 2.

As-rich streams towards the source of thermal water where temperatures reached nearly 40 °C. Several dead larvae were found near the thermal sources.

The other genera of fly larvae were found by the hundreds to thousands living in pH 2–3 non-thermal acid–sulfate water of Alluvium Creek in Brimstone Basin. These were identified as members of the Ephydridae Family and no further identification was made (G.G. Geesy, Montana State University, written communication, 2007). Two analyses of this water also are given in Table 10 and the larvae are shown in Fig. 17.

Ephydrids are known for their ability to adapt under harsh conditions of water composition and for living at low values of pH. *Ephydra thermophila* has been described by Collins (1972) and Brock (1978). It lives in acid habitats, particularly acid algal mats. The ephydrid larvae observed did not develop in algal mats; rather, they were freely wriggling in clear, shallow water.

7. Conclusions

Acid–sulfate waters in Yellowstone National Park, defined as those with pH values below 5, comprise about 36% of thermal waters sampled in the authors' database of 709 samples. All thermal waters are bimodally distributed between acid–sulfate waters and neutral-chloride waters. Further classification of the chemistry of Yellowstone's thermal waters leads to recognition of (1) meteoric waters only (MO) that have dissolved small amounts of solutes through weathering processes at low temperature and have not contacted thermal fluids, (2) meteoric waters that have been heated by high-temperature gases only (MG) usually containing some H_2S that has oxidized to H_2SO_4 achieving high SO_4 concentrations (100–3000 mg/L) and high $\delta^{18}O$ values, (3) deep hydrothermal waters only (HO) with Cl concentrations of 310–400 mg/L and SO_4 concentrations of 10–100 mg/L, (4) deep hydrothermal waters that have boiled at some depth (HB), achieving Cl concentrations greater than 400 mg/L (several hot springs in Norris Geyser Basin are over 600 mg/L and Perpetual Spouter frequently contains over 800 mg/L Cl), (5) hydrothermal waters that have boiled at depth and have been heated further with H_2S-enriched gases (HBG) to achieve higher SO_4 concentrations (Sulphur Spring), (6) mixtures of these previous types (Cistern Spring), and (7) H_2SO_4 formed by the ambient-temperature oxidation of elemental S in hydrothermally altered areas that are no longer thermally active. Some springs undergo extreme changes in chemistry from a neutral-chloride type to an acid–sulfate type in a short time period. Crystal Spring has changed from dominantly an HB-type to dominantly an MG-type within one year.

Acid–sulfate waters in the data base exhibit several characteristics that distinguish them from other acid waters such as acid mine waters and natural acid rock drainage. Although their pH values range from 1.2 to 5 and their SO_4 concentrations can be as high as 6500 mg/L, their SO_4 concentrations are much lower than most acid mine waters at the same pH. This difference results from S oxidation rather than pyrite oxidation, i.e. only 1 mol of H_2SO_4 is formed from 1 mol of S whereas 2 mol of H_2SO_4 and 1 mol of dissolved Fe are formed from one mole of pyrite. Oxidation and hydrolysis of Fe adds more H^+ ions than what is possible from S oxidation alone. Metal concentrations are much lower in acid–sulfate thermal waters than in acid mine waters. As the pH decreases below 3, H^+ becomes the major cation and Fe and Al concentrations are generally an order of magnitude or more less than those in acid mine waters. For these reasons, acidity titrations, when minor hydrolysis reactions are accounted for, can provide a quantitative measure of free H^+ concentration and an independent measure of pH for pH values below 3. Likewise the pH can often be estimated from charge balance at pH values below 3. An important conclusion for QA/QC is that charge balance/imbalance is dependent on a speciation model for these waters when the pH is less than 3.

Sulfate concentrations in HO or HB waters are low (10–100 mg/L) and as this water boils, Cl concentrations increase but SO_4 concentrations decrease. This trend can be explained by decreasing anhydrite solubility equilibrium as the temperature increases, or by removal of dissolved S by H_2S degassing during boiling and decreasing the total dissolved S. Some waters in the SO_4–Cl trend result from mixing but either anhydrite mineral solubility or H_2S degassing is necessary to produce the high-Cl, low-SO_4 endmember.

Certain eukaryotes, i.e. fly larvae, can reproduce in Yellowstone's acid waters of pH 2–3 as shown by observations of Stratiomyidae and Ephrydidae. Because such organisms have never been found in acid mine waters, it can be concluded that it takes more than just acid conditions to limit eukaryotic growth. Quite likely it is the high metal concentrations in acid mine waters that prevent the growth of Diptera.

Acknowledgments

The authors are grateful for the support of the National Research Program of the Water Resources Discipline, USGS, and to the Biotic Surveys and Inventories program of NSF Grant DEB 02030677 awarded to Cristina Tackas-Vesbach and Anna-Louise Reysenbach. We are particularly appreciative of the NPS staff of Yellowstone National Park who have been generous in their time and helpful in all our endeavors to obtain hot water samples in dangerous places. We would like to especially thank the late Rick Hutchinson, past and present research coordinators Ann Deutsch and Christie Hendrix, respectively, Ann Rodman, Steve Miller, and the past and present directors of the Center for Natural Resources, John Varley and Tom Oliff, respectively. Several colleagues, post-docs, and students assisted on field sampling trips including Sara LoVetere, JoAnn Holloway, Yong Xu, Martin Schoonen, Greg Druschel, Corey Cohn, Jennifer DeMonge, Gordon Southam, Chris Knickerbocker, Randy Mielke, Ravin Donald, Bill Stanley, Maria Elvira Hernandez, Britta Planer-Freidrich, Juliane Becker, Beate Böhme, Maria Rosario Pereira, and Maria Pilar Asta. Any use of trade, firm, or product names is for descriptive purposes only and does not imply endorsement by the US Government.

References

American Public Health Association (APHA), 1985. Method 428C. Methylene blue method for sulfide. In: Standard Methods for the Examination of Water and Wastewater (14th ed.). American Public Health Association, pp. 403–405.

Arnórsson, S., 1995. Geothermal systems in Iceland: structure and conceptual models – I. High-temperature areas. Geothermics 24, 561–602.

Arnórsson, S., Grönvold, K., Sigurdsson, S., 1978. Aquifer chemistry of four high-temperature geothermal systems in Iceland. Geochim. Cosmochim. Acta 42, 523–536.

Ball, J.W., Nordstrom, D.K., 1991. User's manual for WATEQ4F, with revised thermodynamic data base and test cases for calculating speciation of major, trace and redox elements in natural waters. US Geol. Surv. Open-File Report 91-183.

Ball, J.W., Nordstrom, D.K., 1994. A comparison of simultaneous plasma, atomic absorption, and iron colorimetric determinations of major and trace constituents in acid mine waters. US Geol. Surv. Water-Resour. Invest. Report 93-4122.

Ball, J.W., McCleskey, R.B., Nordstrom, D.K., Holloway, J.M., 2007. Water-chemistry data for selected springs, geysers, and streams in Yellowstone National Park, Wyoming, 2003–2005. US Geol. Surv. Open-File Report 2006-1339. p. 183.

Ball, J.W., McCleskey, R.B., Nordstrom, D.K., Holloway, J.M., Verplanck, P.L., 2002. Water-chemistry data for selected springs, geysers, and streams in Yellowstone National Park, Wyoming, 1999–2000. US Geol. Surv. Open-File Report 02-382.

Ball, J.W., Nordstrom, D.K., Cunningham, K.M., Schoonen, M.A.A., Xu, Y., DeMonge, J.M., 1998b. Water-chemistry and on site sulfur-speciation data for selected springs in Yellowstone National Park, Wyoming, 1994–1995. US Geol. Surv. Open-File Report 98-574.

Ball, J.W., Nordstrom, D.K., Jenne, E.A., Vivit, D.V., 1998a. Chemical analyses of hot springs, pools, geysers, and surface waters from Yellowstone National Park, Wyoming, and vicinity, 1974–1975. US Geol. Surv. Open-File Report 98-182.

Ball, J.W., Nordstrom, D.K., McCleskey, R.B., Schoonen, M.A.A., Xu, Y., 2001. Water-chemistry and on site sulfur-speciation data for selected springs in Yellowstone National Park, Wyoming, 1996–1998. US Geol. Surv. Open-File Report 01-49.

Barnard, W.R., Nordstrom, D.K., 1980. Fluoride in precipitation-I. Methodology with the fluoride-selective electrode.. Atmos. Environ. 16, 99–103.

Barringer, J.L., Johnsson, P.A., 1996. Theoretical considerations and a simple method for measuring alkalinity and acidity in low-pH waters by Gran titration. US Geol. Surv. Water-Resour. Invest. Report 89-4029.

Baumann, E.W., 1974. Determination of parts per billion sulfide in water with the sulfide-selective electrode. Anal. Chem. 46, 1345–1347.

Brinton, T.I., Antweiler, R.C., Taylor, H.E., 1995. Method for the determination of dissolved chloride, nitrate, and sulfate in natural water using ion chromatography. US Geol. Surv. Open-File Report 95-426A.

Brown, E., Skougstad, M.W., Fishman, M.D., 1970. Methods for collection and analyses of water samples for dissolved minerals and gases. US Geol. Surv. Tech. Water Resour. Invest., Book 5 (Chapter A1).

Brock, T.D., 1971. Bimodal distribution of pH values of thermal springs of the world. Bull. Geol. Soc. Am. 82, 1393–1394.

Brock, T.D., 1978. Thermophilic Microorganisms and Life at High Temperatures. Spring-Verlag.

Burnham, C.W., Ohmoto, H., 1980. Late stage processes of felsic magmatism. Soc. Min. Geol. Jap. Spec. Issue 8, 1–11.

Charlton, S.R., Macklin, C.L., Parkhurst, D.L., 1997. PHREEQCI – a graphical user interface for the geochemical computer program PHREEQC. US Geol. Surv. Water-Resour. Invest. Report 97-4222.

Clegg, S.L., Rard, J.A., Pitzer, K.S., 1994. Thermodynamic properties of 0–6 mol kg^{-1} aqueous sulfuric acid from 273.15 to 328.15 K. J. Chem. Soc. Faraday Trans. 90, 1875–1894.

Collins, N.C., 1972. Population ecology of the brine fly *Ephydra thermophila* (Diptera: Ephydridae) associated with acid seepages in Yellowstone National Park, Wyoming. Ph.D. Dissertation, Univ. Georgia, Athens.

Coplen, T.B., 1994. Reporting of stable hydrogen, carbon, and oxygen isotopic abundances. Pure Appl. Chem. 66, 273–276.

Coplen, T.B., Wildman, J.D., Chen, J., 1991. Improvements in the gaseous hydrogen-water equilibrium technique for hydrogen isotope ratio analysis. Anal. Chem. 63, 910–912.

Craig, H., 1963. The isotopic geochemistry of water and carbon in geothermal area. In: Tongiorgi, E. (Ed.), Nuclear Geology on Geothermal Areas, Spoleto, Consiglio Nazionale delle Ricerche. laboratorio di Geologia Nucleare, Pisa, pp. 7–53.

DeWild, J.F., Olsen,M.L., Olund, S.D., 2002. Determination of methyl mercury by aqueous phase ethylation, followed by gas chromatographic separation with cold vapor atomic fluorescence detection. US Geol. Surv. Open-File Report 2001-445.

Druschel, G.K., Schoonen, M.A.A., Nordstrom, D.K., Ball, J.W., Xu, Yong, Cohn, C.A., 2003. Sulfur geochemistry of hydrothermal waters in Yellowstone National Park, Wyoming, USA. III. An anion-exchange resin technique for sampling and preservation of sulfoxyanions in natural waters. Geochem. Trans. 4, 12–19.

DVWK, 1990. Methodsammlung zur Auswertung und Darstellung von Grundwasserbeschaffenheitsdaten. Verlag Paul Parey.

Einaudi, M.T., Hedenquist, J.W., Inan, E.E., 2003. Sulfidation state of fluids in active and extinct hydrothermal systems: transitions from porphyry to epithermal environments. In: Simmons S.F., Graham, I. (Eds.), Volcanic, Geothermal, and Ore-Forming Fluids: Rulers and Witnesses of Processes within the Earth, Soc. Econ. Geol. Spec. Publ. No. 10, pp. 285–313 (Chapter 15).

Ellis, A.J., Mahon, W.A.J., 1977. Chemistry and Geothermal Systems. Academic Press, New York.

Epstein, S., Mayeda, T., 1953. Variation of O^{18} content of water from natural sources. Geochim. Cosmochim. Acta 4, 213–224.

Fishman, M.J., Friedman, L.C., 1985. Methods for determination of inorganic substances in water and fluvial sediments. Tech. Water Resour. Invest. U.S. Geol. Surv., Book 5, Open-File Report 85-495 (Chapter A1).

Fournier, R.O., 2006. Geochemistry and dynamics of Yellowstone National Park hydrothermal system. In: Inskeep, W.P., McDermott, T.R. (Eds.), Geothermal

Biology and Geochemistry in Yellowstone National Park. Thermal Biology Institute, Montana State University, Bozeman, MT, pp. 3–29.
Fournier, R.O., Thompson, J.M., Hutchinson, R.A., 1986. Fluctuations in composition of Cistern Spring, Norris Geyser Basin, Yellowstone National Park, WY – variable boiling and mixing 1962–1985. In: Extended Abstract, 5th Internat. Symp. Water–Rock Interaction, Reykjavik, Iceland, pp. 206–209.
Fournier, R.O., Weltman, U., Counce, D., White, L.D., Janik, C.J., 2002. Results of weekly chemical and isotopic monitoring of selected springs in Norris Geyser Basin, Yellowstone National Park during June–September, 1995. US Geol. Surv. Open-File Report 02-344.
Garbarino, J.R., Taylor, H.E., 1979. An inductively coupled plasma atomic emission spectrometric method for routine water quality testing. Appl. Spectr. 33, 220–226.
Giggenbach, W.F., 1971. Isotopic composition of waters of the Broadlands geothermal field (New Zealand). N. Z. J. Sci. 14, 959–970.
Giggenbach, W.F., 1978. The isotopic composition of waters from the El Tatio geothermal field, northern Chile, Geochim. Cosmochim. Acta 42, 979–988.
Giggenbach, W.F., 1988. Geothermal solute equilibria. Deviation of the Na–K–Mg–Ca geoindicators. Geochim. Cosmochim. Acta 52, 2749–2765.
Giggenbach, W.F., 1997. The origin and evolution of fluids in magmatic-hydrothermal systems. In: Barnes, H.L. (Ed.), Geochemistry of Hydrothermal Ore Deposits, third ed. John Wiley & Sons, pp. 737–796.
Holland, H.D., 1965. Some applications of thermochemical data to problems of ore deposits. II. Mineral assemblages and the composition of ore-forming fluids. Econ. Geol. 60, 1101–1166.
Holland, H.D., 1967. Gangue minerals in hydrothermal ore deposits. In: Barnes, H.L. (Ed.), Geochemistry of Hydrothermal Ore Deposits, Holt, Rinehart. Winston, New York, pp. 382–436.
Hölting, B., 1996. Hydrogeologie.-5 Aufl, Enke.
Horvat, M., Bloom, N.S., Liang, L., 2003. Comparison of distillation with other current isolation methods for the determination of methyl mercury compounds in low level environmental samples. Part 1. Sediments. Anal. Chim. Acta 281, 135–152.
Johnson, D.L., Pilson, M.E.Q., 1972. Spectrophotometric determination of arsenite, arsenate, and phosphate inn natural waters. Anal. Chim Acta 58, 289–299.
Johnson, G.W., Taylor, H.E., Skogerboe, R.K., 1979. Determination of trace elements in natural waters by the direct current plasma, multielement- atomic emission spectrometer (DCP-MAES) technique. Spectrochim. Acta 34B, 197.
Kameda, M., 1963. Volcano and geothermics at Iwojima, Kagoshima-ken. Jinetsu 3, 1–23.
Kennedy,V.C., Jenne, E.A., Burchard, J.M., 1976. Backflushing filters for field processing of water samples prior to trace-element analyses. US Geol. Surv. Open-file Report 76-126.
Kharaka, Y.K., Thordsen, J.J., White, L.D., 2002. Isotope and chemical compositions of meteoric and thermal waters and snow from the greater Yellowstone National Park region. US Geol. Surv. Open-File Report 02-194.
Kirby, C., Cravotta III, C.A., 2005a. Net alkalinity and net acidity 1: theoretical considerations. Appl. Geochem. 20, 1920–1940.
Kirby, C., Cravotta III, C.A., 2005b. Net alkalinity and net acidity 2: practical considerations. Appl. Geochem. 20, 1941–1964.
Langford, N.P., 1905. The Discovery of Yellowstone Park: Journal of the Washburn Expedition to the Yellowstone and Firehole Rivers in the Year 1870. Reproduced in 1972. University of Nebraska Press.
Mariner, R.H., Presser, T.S., Evans, W.E., 1993. Geothermometry and water-rock interaction in selected thermal systems in the Cascade Range and Modoc Plateau, western United States. Geothermics 22, 1–15.
Marini, L., Vetuschi Zuccolini, M., Saldi, G., 2003. The bimodal pH distribution of volcanic lake waters. J. Volcanol. Geotherm. Res. 121, 83–98.
McCleskey, R.B., Ball, J.W., Nordstrom, D.K., Holloway, J.M., Taylor, H.E., 2005. Water-chemistry data for selected hot springs, geysers, and streams in Yellowstone National Park, Wyoming, 2001–2002. US Geol. Surv. Open-File Report 2004-1316.
McCleskey, R.B., Nordstrom, D.K., Ball, J.W., 2003. Metal interferences and their removal prior to the determination of As(T) and As(III) in acid mine waters by hydride generation atomic absorption spectrometry. US Geol. Surv. Water-Resour. Invest. Report 2003-4117.
Moses, C.O., Nordstrom, D.K., Mills, A.L., 1984. Sampling and analysing mixtures of sulphate sulphite, thiosulphate and polythionate. Talanta 1, 331–339.
Mottl, M.J., Holland, H.D., 1978. Chemical exchange during hydrothermal alteration of basalt by seawater – I. Experimental results for major and minor components of seawater. Geochim. Cosmochim. Acta 42, 1103–1115.
Nordstrom, D.K., 1977. Thermochemical redox equilibria of ZoBell's solution. Geochim. Cosmochim. Acta 41, 1835–1841.
Nordstrom, D.K., Archer, D.G., 2003. Arsenic thermodynamic data and environmental geochemistry. In: Welch, A.H., Stollenwerk, K.G. (Eds.), Arsenic in Ground Water. Kluwer Publishers, Amsterdam, pp. 1–6.
Nordstrom, D.K., Munoz, J.L., 1994. Geochemical Thermodynamics, second ed. Blackwell Scientific Publications, Boston, MA.
Ohmoto, H., Goldhaber, M.B., 1997. Sulfur and carbon isotopes. In: Barnes, H.L. (Ed.), Geochemistry of Hydrothermal Ore Deposits, third ed. John Wiley & Sons, pp. 517–612.
Panichi, C., Gonfiantini, R., 1981. Geothermal waters. In: Gat, J.R., Gonfiantini, R. (Eds.), Stable Isotope Hydrology, Deuterium and Oxygen-18 in the Water Cycle. IAEA Tech. Report Series 210, pp. 241–271.
Parkhurst, D.L., Appelo, C.A.J., 1999. User's guide to PHREEQC (version 2) – A computer program for speciation, batch-reaction, one-dimensional transport, and inverse geochemical calculations. US Geol. Surv. Water-Resour. Invest. Report 99-4259.
Plumlee, G.S., Smith, K.S., Montour, M.R., Ficklin, W.H., Mosier, E.L., 1999. Geologic controls on the composition of natural waters and mine waters draining diverse mineral-deposit types. In: Filipek, L.H., Plumlee, G.S. (Eds.), The Environmental Geochemistry of Mineral Deposits, 6B, Case Studies and Research Topics, pp. 373–432.
Raymahashay, B.C., 1968. A geochemical study of rock alteration by hot springs in the Paint Pot Hill area, Yellowstone Park. Geochim. Cosmochim. Acta 32, 499–522.
Revesz, K., Coplen, T.B., 2003a. Hydrogen isotope ratio analysis of water by gaseous hydrogen–water equilibration. Standard Operating Procedure #1574, Techniques of the US Geol. Survey.
Revesz, K., Coplen, T.B., 2003b. Oxygen isotope ratio analysis of water by gaseous carbon dioxide–water equilibration. Standard Operating Procedure #499, Techniques of the US Geol. Survey.
Rodman, A., Guiles, C., 2008. Greater Yellowstone Science Learning Center and the Yellowstone Thermal Inventory. In: Inskeep, W., Peters, J. (Eds.), Geothermal Biology and Geochemistry in Yellowstone National Park. NSF Research Coordination Network and Montana State University Thermal Biology Institute 2008 Workshop, January 10–13.
Roth, D.A., Taylor, H.E., Domagalski, J., Dileanis, P., Peart, D.B., Antweiler, R.C., Alpers, C.N., 2001. Distribution of inorganic mercury in Sacramento River water and sediments. Arch. Environ. Contam. Toxicol. 40, 161–172.
Rye, R.O., 1993. The evolution of magmatic fluids in the epithermal environment: the stable isotope perspective. Econ. Geol. 88, 733–752.
Rye, R.O., Truesdell, A.F., 1993. The question of recharge to the geysers and hot springs of Yellowstone National Park. US Geol. Surv Open-File Report 93-384.
Sakai, H., Matsubaya, O., 1977. Stable isotope studies of Japanese geothermal systems. Geothermics 9, 97–124.
Seyfried Jr., W.E., Bischoff, J.L., 1981. Experimental seawater–basalt interaction at 300 °C, 500 bars, chemical exchange, secondary mineral formation and implications for the transport of heavy metals. Geochim. Cosmochim. Acta 45, 135–147.
Southam, G., Donald, R., Nordstrom, D.K., Ball, J.W., 1997. Biogeochemistry of natural elemental sulfur oxidation and derivative acidic waters at Brimstone Basin, Yellowstone National Park, Wyoming: II. Microbiological results. Geol. Soc. Am. Abstracts with Programs 29, 6, A 297.
Stoffregen, R.E., Alpers, C.N., Jambor, J.L., 2000. Alunite-jarosite crystallography, thermodynamics, and geochronology. In: Alpers, C.N., Jambor, J.L., Nordstrom, D.K. (Eds.), Sulfate Minerals. Rev. Mineral. Geochem. 40, 454–479.
Stookey, L.L., 1970. Ferrozine – a new spectrophotometric reagent for iron. Anal. Chem. 42, 779–781.
Taylor, H.E., 1978. Atomic absorption spectrometry. In: Skougstad, M.W., Fishman, M.J., Friedman, L.C., Erdmann, D.E., Duncan, S.S. (Eds), Methods for Analysis of Inorganic Substances in Water Fluvial Sediments. US Geol. Surv. Open-File Report No. 78-679.
Taylor, H.E., 2001. Inductively Coupled Plasma-Mass Spectrometry. Practices and Techniques. New York, Academic Press, New York.
Taylor, H.E., Berghoff, K., Andrews, E.D., Antweiler, R.C., Brinton, T.I., Miller, C., Peart, D.B., Roth, D.A., 1997. Water Quality of Springs and Seeps in Glen Canyon National Recreation Area. National Park Service Technical Report NPS/NRWRD/NRTR-97/128.
Thompson, J.M., DeMonge, J.M., 1996. Chemical analyses of hot springs, pools, and geysers from Yellowstone National Park, Wyoming, and vicinity, 1980–1993. US Geol. Surv. Open-File Report 96-68.
To, T.B., Nordstrom, D.K., Cunningham, K.M., Ball, J.W., McCleskey, R.B., 1999. New method for the direct determination of dissolved Fe(III) concentration in acid mine waters. Environ. Sci. Technol. 33, 807–813.
Truesdell, A.H., Huston, J.R., 1980. Isotopic evidence on environments of geothermal systems. In: Fritz, P., Fontes, J.-C. (Eds.), Handbook of Environmental Isotope Geochemistry, vol. 1, pp.179–226.
Truesdell, A.H., Rye, R.O., Whelan, J.F., Thompson, J.M., 1978. Sulfate chemical and isotopic patternsn in thermal waters of Yellowstone National Park, Wyoming. Short papers of the further international conference, geochronology, cosmochronology, isotope geology 1978, US Geol. Surv. Open-File Report 78-801, pp. 435–436.
Wexler, A.S., Clegg, S.L., 2002. Atmospheric aerosol models for systems including the ions H^+, NH_4^+, Na^+, SO_4^{2-}, NO_3^-, Cl^-, Br^-, and H_2O. J. Geophys. Res.-Atmos. 107, 4207–4218.
White, D.E., 1957. Thermal waters of volcanic origin. Bull. Geol. Soc. Am. 68, 1637–1658.
White, D.E., Hutchinson, R.A., Keith, T.E.C., 1988. The geology and remarkable thermal activity of Norris Geyser Basin, Yellowstone National Park, Wyoming. US Geol. Surv. Prof. Paper 1456.
Xu, Y., Schoonen, M.A.A., Nordstrom, D.K., Cunningham, K.M., Ball, J.W., 1998. Sulfur geochemistry of hydrothermal waters in Yellowstone National Park: I. The origin of thiosulfate in hot spring waters. Geochim. Cosmochim. Acta 62, 3729–3743.
Xu, Y., Schoonen, M.A.A., Nordstrom, D.K., Cunningham, K.M., Ball, J.W., 2000. Sulfur geochemistry of hydrothermal waters in Yellowstone National Park, Wyoming, USA: II. Formation and decomposition of thiosulfate and polythionate in Cinder Pool. J. Volcanol. Geotherm. Res. 97, 407–423.